Establishment and maintenance of motor neuron identity via temporal modularity in terminal selector function

Yinan Li [1, 2], Anthony Osuma [1, 2], Edgar Correa [1, 3], Munachiso A. Okebalama[1], Pauline Dao[1], Olivia Gaylord [4], Jihad Aburas [1], Priota Islam [5, 6], André E.X. Brown [5, 6], Paschalis Kratsios [1, 2, 3, 4, 7]

[1] Department of Neurobiology, University of Chicago, Chicago, IL, USA

[2] Committee on Neurobiology, University of Chicago, Chicago, IL, USA

[3] Cell and Molecular Biology Program, University of Chicago, Chicago, IL, USA

[4] Committee on Development, Regeneration and Stem Cell Biology, University of Chicago, Chicago, IL, USA

[5] MRC London Institute of Medical Sciences, London, UK

[6] Institute of Clinical Sciences, Imperial College London, London, UK

[7] The Grossman Institute for Neuroscience, Quantitative Biology, and Human Behavior, University of Chicago, Chicago, IL, USA

Correspondence: pkratsios@uchicago.edu

ABSTRACT (150 words)

Terminal selectors are transcription factors (TFs) that establish during development and maintain throughout life post-mitotic neuronal identity. We previously showed that UNC-3/Ebf, the terminal selector of *C. elegans* cholinergic motor neurons (MNs), acts indirectly to prevent alternative neuronal identities (Feng et al., 2020). Here, we globally identify the direct targets of UNC-3. Unexpectedly, we find that the suite of UNC-3 targets in MNs is modified across different life stages, revealing "temporal modularity" in terminal selector function. In all larval and adult stages examined, UNC-3 is required for continuous expression of various protein classes (e.g., receptors, transporters) critical for MN function. However, only in late larvae and adults, UNC-3 is required to maintain expression of MN-specific TFs. Minimal disruption of UNC-3's temporal modularity via genome engineering affects locomotion. Another *C. elegans* terminal selector (UNC-30/Pitx) also exhibits temporal modularity, supporting the potential generality of this mechanism for the control of neuronal identity.

INTRODUCTION

Nervous system development is a multi-step process that culminates in the generation of distinct neuron types necessary for animal behavior. Seminal studies in many model systems have begun to elucidate the molecular mechanisms that control the early steps of neuronal development, such as specification of neural progenitors and generation of post-mitotic neurons (Catela and Kratsios, 2019, Doe, 2017, Greig et al., 2013, Jessell, 2000, Lodato and Arlotta, 2015, Perry et al., 2017). However, our understanding of the final steps of neuronal development is very rudimentary. Once neurons become post-mitotic, how do they acquire their unique functional features, such as neurotransmitter synthesis, electrical activity and signaling properties? And, perhaps more importantly, how do neurons maintain such features throughout post-embryonic life?

Terminal selectors represent one class of transcription factors (TFs) with continuous expression – from development through adulthood – in specific neuron types (Hobert, 2008, Hobert, 2011, Hobert, 2016b, Garcia-Bellido, 1975). A defining feature of terminal selectors is the ability to activate the expression of effector genes, whose protein products determine the terminally differentiated state, and thereby function, of a given neuron type. Such effector genes, herein referred to as “terminal identity genes”, are expressed continuously in specific neuron types and endow them with distinct functional and phenotypic properties. Examples include neurotransmitter (NT) biosynthesis components, NT receptors, ion channels, neuropeptides, and adhesion molecules (Hobert, 2008, Hobert, 2011, Hobert, 2016b). Numerous studies support the idea that terminal selectors establish during development and maintain throughout life neuronal identity (and function) by activating expression of terminal identity genes (Deneris and Hobert, 2014, Hobert, 2008, Hobert, 2016b, Hobert and Kratsios, 2019). Multiple cases of terminal selectors have been described thus far in worms, flies, chordates and mice (Deneris and Hobert, 2014, Hobert and Kratsios, 2019, Konstantinides et al., 2018), suggesting high conservation of this type of regulators. Importantly, human mutations in terminal selectors and their effector target genes have been linked to either developmental or degenerative conditions of the nervous system (Deneris and Hobert, 2014).

However, the molecular mechanisms through which terminal selectors establish and maintain neuronal identity are poorly understood, in part due to two major challenges. First, the majority of studies follow a candidate approach focused on a

select subset of terminal identity genes (Flames and Hobert, 2009, Hobert, 2016a, Lopes et al., 2012). Hence, the extent of terminal identity features and breadth of biological processes controlled by terminal selectors remain largely unknown. Addressing this knowledge gap requires unbiased methods for the identification of terminal selector target genes, but such approaches have only been applied to a limited number of terminal selectors to date (Corbo et al., 2010, Housset et al., 2013, Kadkhodaei et al., 2013, Wyler et al., 2016, Yu et al., 2017). Second, the continuous expression of terminal selectors represents an additional challenge because it is not known whether their function - in a particular neuron type - remains the same, or changes at different life stages. This is partly due to the difficulty of tracking individual neurons in the complex vertebrate nervous system throughout embryonic and post-natal life. Hence, longitudinal studies in simple model organisms are needed to determine whether terminal selectors control an identical suite of target genes across different stages (e.g., embryo, adult), or whether the suite of targets can change over time. Addressing these two challenges may extend our knowledge of how terminal selectors control neuronal identity, as well as advance our understanding of how cellular identity is established and maintained.

This study focuses on UNC-3, the sole *C. elegans* ortholog of the Collier/Olf/Ebf (COE) family of TFs (Dubois and Vincent, 2001). UNC-3 acts as a terminal selector in cholinergic motor neurons (MNs) of the *C. elegans* ventral nerve cord (Kratsios et al., 2012). Importantly, mutations in EBF3, a human ortholog of UNC-3, cause a neurodevelopmental syndrome characterized by motor developmental delay (Blackburn et al., 2017, Chao et al., 2017, Harms et al., 2017, Sleven et al., 2017). A previous study proposed that UNC-3 controls cholinergic MN identity in *C. elegans* by activating directly the expression of various terminal identity genes (e.g., acetylcholine biosynthesis components, ion channels, NT receptors, neuropeptides), which were identified via a candidate approach (Kratsios et al., 2012). More recently, it was demonstrated that UNC-3 can also act indirectly to prevent the adoption of alternative neuronal identities (Feng et al., 2020). Lastly, animals lacking *unc-3* gene activity display severe locomotion defects (Brenner, 1974, Feng et al., 2020), suggesting UNC-3 may broadly control gene expression in cholinergic MNs. However, an unbiased identification of UNC-3 targets, as well as a longitudinal analysis of *unc-3* mutants are currently lacking.

Here, we employ chromatin immunoprecipitation followed by DNA sequencing (ChIP-Seq) and report the identification of ~3,500 protein-coding genes as putative direct targets of UNC-3. Protein class ontology analysis suggests that UNC-3, besides terminal identity genes, also controls additional biological processes, such as neuronal metabolism and downstream gene regulatory networks comprised of numerous TFs and nucleic acid-binding proteins. These findings help obtain a comprehensive understanding of terminal selector function.

Through a longitudinal analysis of *unc-3* mutants at embryonic, larval and adult stages, we identified two groups of target genes with distinct temporal requirements for UNC-3 in cholinergic MNs. One group encodes multiple classes of proteins (e.g., receptors, secreted molecules, TFs) that require UNC-3 for both embryonic initiation and post-embryonic maintenance of their expression. Contrasting this stable mode of regulation over time, a second group of targets consists exclusively of TFs (*cfi-1/Arid3a, bnc-1/BNC1-2, mab-9/Tbx20, ceh-44/CUX1-2, nhr-40/nuclear hormone receptor*) that do not require UNC-3 for initiation, but depend on UNC-3 activity for maintenance. Hence, the suite of UNC-3 targets in cholinergic MNs is modified across different life stages, a phenomenon we term “temporal modularity” in terminal selector function. To provide mechanistic insights, we focused on the second group of targets and identified a molecular mechanism for their *unc-3*-independent initiation that relies on Hox proteins. Importantly, preventing UNC-3’s ability to selectively maintain expression of a single TF (*cfi-1/Arid3a*) from the second target group led to locomotion defects, indicating minimal disruption of temporal modularity affects animal behavior. Lastly, we provide evidence for temporal modularity in the function of UNC-30/PITX, the terminal selector of GABAergic MN identity in *C. elegans* (Eastman et al., 1999, Jin et al., 1994). Because terminal selectors have been identified in both invertebrate and vertebrate nervous systems (Deneris and Hobert, 2014, Hobert and Kratsios, 2019), we hypothesize that temporal modularity in their function may be a general mechanism for the establishment and maintenance of neuronal identity.

138 **RESULTS**

139 **Identifying the global targets of UNC-3 via ChIP-Seq**

140 To identify in an unbiased manner putative UNC-3 target genes, we employed
141 chromatin immunoprecipitation followed by DNA sequencing (ChIP-Seq). We used a
142 reporter strain with in-frame GFP sequences inserted immediately upstream of the stop
143 codon of the endogenous *unc-3* gene (**Figure 1A**). Expression of UNC-3::GFP fusion
144 protein was observed in the nucleus of 53 cholinergic MNs (SAB subtype = 3 neurons,
145 DA = 9, DB = 7, VA = 12, VB = 11, AS = 11) and 19 other neurons known to express
146 *unc-3* (**Figure 1A**), indicating that this reporter faithfully recapitulates the endogenous
147 *unc-3* expression pattern (Pereira et al., 2015, Prasad et al., 1998). Insertion of GFP
148 does not detectably alter the function of UNC-3 since expression of known UNC-3
149 targets (*cho-1/ChT, unc-17/VAChT, ace-2/AChE*) is unaffected in *unc-3::gfp* animals
150 (**Figure 1B**). Unlike *unc-3* null mutants, *unc-3::gfp* animals do not display locomotion
151 defects. We therefore performed ChIP-seq on *unc-3::gfp* animals at larval stage 2 (L2)
152 because all *unc-3* expressing neurons have been generated by this stage.

153 Our ChIP-seq dataset revealed strong enrichment of UNC-3 binding in the
154 genome by identifying a total of 6,892 unique binding peaks (q-value cutoff: 0.05)
155 (**Figure 1C** and **Figure 1 – figure supplement 1**). The majority of UNC-3 binding peaks
156 (91.95%) are predominantly located between 0 and 3 kb upstream of a transcription
157 start site (Kadkhodaei et al.), whereas only a small fraction is found in introns (2.05 %)
158 or downstream of a gene (0.99%), suggesting UNC-3 chiefly acts at promoters and
159 enhancers to regulate gene expression (**Figure 1D** and **1F**). Through *de novo* motif
160 discovery analysis (see Materials and Methods), we identified a 12 bp pseudo-
161 palindromic sequence overrepresented in the UNC-3 binding peaks (**Figure 1E**), which
162 highly resembles the binding site of UNC-3 vertebrate orthologs (Treiber et al., 2010a,
163 Treiber et al., 2010b, Wang and Reed, 1993, Wang et al., 1997). To test the quality of
164 our ChIP-Seq results, we sought to determine whether UNC-3 binding peaks are
165 present in the *cis*-regulatory region of all previously described UNC-3 targets in
166 cholinergic MNs, because these neurons constitute the majority of *unc-3*-expressing
167 cells (53 out of 72 cells). Previous studies identified 10 terminal identity genes as
168 putative direct UNC-3 targets and 43 terminal identity genes whose expression is
169 affected by genetic removal of *unc-3* (Kratsios et al., 2015, Kratsios et al., 2012). In the
170 current study, we found UNC-3 binding peaks in 9 out of 10 (90%) direct UNC-3 targets

171 and 38 of the 43 (88.37%) downstream targets of UNC-3, indicating high quality in the
172 ChIP-Seq results (**Figure 2A** and **Figure 1 – figure supplement 1, Supplementary**
173 **File 1**). Moreover, ChIP-Seq for UNC-3 appears highly sensitive, as it identified peaks in
174 *unc-3*-dependent genes expressed in a limited number neurons (e.g., *glr-4/GluR* is
175 expressed in 4 out of 72 *unc-3*+ neurons) (**Figure 2A**). In conclusion, our ChIP-Seq
176 experiment generated a comprehensive map of UNC-3 binding in the *C. elegans*
177 genome and provided biochemical evidence to the hypothesis that UNC-3 binds to the
178 *cis*-regulatory region of multiple terminal identity genes, consolidating UNC-3's function
179 as a terminal selector of cholinergic MN identity.
180 Our bioinformatic analysis of the UNC-3 binding peaks revealed 3,502 protein-
181 coding genes as putative UNC-3 targets (see Materials and Methods). To classify these
182 new targets, we performed gene ontology (GO) analysis focused on protein classes
183 using PANTHER (Mi et al., 2013). This analysis revealed three broad categories
184 (**Figure 2B, Supplementary File 2**). First, there is a preponderance (42.18 % of the
185 total number of UNC-3 targets classified by PANTHER) of terminal identity genes (e.g.,
186 114 transporter proteins, 111 receptors and trans-membrane proteins, 37 signaling
187 molecules, 11 cell adhesion molecules), suggesting that UNC-3 broadly affects multiple
188 features of neuronal terminal identity. The second overrepresented category (24.07% of
189 UNC-3 targets) contains a large number of proteins involved in the control of gene
190 expression, such as 239 nucleic acid binding proteins (16.77 %) and 104 TFs (7.3 %),
191 highlighting the possibility of an extensive network of gene regulatory factors
192 downstream of UNC-3. The third category (24.14 %) consists of genes coding for
193 various types of enzymes (e.g., hydrolases, ligases, oxidoreductases), suggesting a
194 new role for UNC-3 in neuronal metabolic pathways. Together, this analysis unravels
195 the breadth of biological processes potentially under the direct control of UNC-3.
196 The ChIP-Seq experiment was performed on endogenously tagged UNC-3, which
197 is expressed in 53 cholinergic MNs of the nerve cord and 19 other neurons located in
198 the *C. elegans* head and tail (Pereira et al., 2015). Since MNs are the majority (53 cells)
199 of *unc-3*-expressing cells (72 in total), a significant portion of the UNC-3-bound genes
200 may be expressed in MNs. To test this, we used available single-cell RNA-Seq data
201 (CeNGEN project: www.cengen.org) that identified 576 transcripts specifically enriched
202 in cholinergic MNs (Seth R Taylor, 2019). We found that 52.95% of these MN-
203 expressed genes are bound by UNC-3 and fall in the aforementioned gene categories

204 (**Supplementary File 3**), thereby constituting putative UNC-3 targets in cholinergic
205 MNs.
206
207 ***Cis*-regulatory analysis reveals novel TFs as direct UNC-3 targets in motor**
208 **neurons**
209 Our ChIP-Seq results provide an opportunity to reveal new roles for UNC-3, beyond the
210 direct control of terminal identity genes. To this end, we focused on the 104 TFs
211 identified by ChIP-Seq as putative UNC-3 targets (**Figure 2B-C**). To functionally test
212 whether the UNC-3 bound DNA elements upstream of these TF-encoding genes carry
213 information critical for gene expression, we carried out a *cis*-regulatory analysis. We
214 isolated and fused to RFP 15 elements located upstream of 15 randomly selected TFs
215 of different families (e.g., homeobox, nuclear hormone receptors, Zn finger) (**Figure 2C,**
216 **Table 1**). We generated transgenic reporter animals and found that 10 of these *cis*-
217 regulatory elements were sufficient to drive RFP expression in ventral cord cholinergic
218 MNs (**Table 1**). Expression of five TFs (*nhr-1, nhr-19, nhr-49, zfh-2, ztf-26*) in ventral
219 cord MNs has not been previously described. The remaining 5 TFs (*cfi-1/Arid3a*, *bnc-*
220 *1/Bnc1/2*, *mab-9/Tbx20*, *nhr-40*, *ceh-44/Cux1)* are known to be expressed in subsets of
221 *unc-3*-positive MNs (Kerk et al., 2017, Pocock et al., 2008, Brozova et al., 2006), but our
222 analysis revealed the *cis*-regulatory elements that are sufficient for their MN expression.
223 Of note, some of these TF reporters are also expressed in *unc-3*-negative MNs of the
224 nerve cord, namely the GABAergic DD and VD neurons (**Table 1**). Next, we tested for
225 *unc-3* dependency at the L4 stage, and found that 9 of these 10 TF reporters depend on
226 *unc-3* for proper expression in cholinergic MNs (**Table 1**). Eight reporters (*nhr-1, nhr-40,*
227 *zfh-2, ztf-26, ceh-44, cfi-1, bnc-1, mab-9)* are positively controlled by *unc-3,* whereas
228 one (*nhr-49*) is negatively regulated by *unc-3* (**Figure 3 – figure supplement 1, Table**
229 **1**). Together, this *cis*-regulatory analysis revealed novel TFs as direct UNC-3 targets in
230 cholinergic MNs. Besides its known role as an activator of terminal identity genes
231 (Kratsios et al., 2015, Kratsios et al., 2012), these findings suggest that UNC-3 can also
232 act directly to either activate or repress expression of multiple TF-encoding genes,
233 uncovering an extensive gene regulatory network downstream of UNC-3.
234
235 **Temporal modularity of UNC-3 function in cholinergic motor neurons**
236 Terminal selectors are continuously expressed, from development through adulthood, in

specific neuron types. However, it remains unclear whether – in the same neuron type – a terminal selector controls an identical suite of targets across different life stages, or the suite of targets can change over time. The case of UNC-3 offers an opportunity to address this issue because its direct targets (terminal identity genes and newly identified TFs [**Table 1**]) are continuously expressed in cholinergic MNs. However, *unc-3* dependency of terminal identity genes was mostly tested at a single developmental stage, the last larval stage (L4) (Kratsios et al., 2012). We therefore performed a longitudinal analysis to determine whether target gene dependency on *unc-3* remains stable or changes at different life stages.

First, we tested 4 terminal identity genes (*acr-2/AChR*, *unc-129/TGFbeta*, *glr-4/GluR*, *unc-17/VAChT*) at larval (L2, L4) and adult (day 1) stages and found that their MN expression, at every stage, critically depends on UNC-3 (**Figure 3A**). However, a different picture emerged after testing the 8 TF reporters that are positively regulated by UNC-3 (**Table 1**). Similar to terminal identity genes, the expression of 3 TFs (*zfh-2/Zfhx3, ztf-26, nhr-1*) critically depends on UNC-3 at every stage (L2, L4, adult) (**Figure 3 – figure supplement 1**), suggesting UNC-3 controls initiation and maintenance of their expression. In striking contrast, the early expression (L2 stage) of five TFs (*cfi-1, bnc-1, mab-9, nhr-40, ceh-44*) does not require UNC-3 (**Figure 3B**). However, maintenance of their expression during late larval and/or adult stages does depend on UNC-3 (**Figure 3B**). Hence, this longitudinal analysis revealed two groups of targets with distinct requirements for UNC-3 at different life stages. One group consists of terminal identity genes (*acr-2/AChR*, *unc-129/TGFbeta*, *glr-4/GluR*, *unc-17/VAChT*) and TFs (*zfh-2/Zfhx3, ztf-26, nhr-1*) that require UNC-3 for both initiation and maintenance of expression ("initiation and maintenance" module, **Figure 3A, C**). The second group consists exclusively of TFs (*cfi-1/Arid3a, bnc-1/Bnc1, mab-9/Tbx20, ceh-44/Cux1, nhr-40*) that depend on UNC-3 for maintenance, but not initiation ("maintenance-only" module, **Figure 3B-C**).

Collectively, these findings suggest that, in cholinergic MNs, the suite of UNC-3 target genes can change at different life stages; distinct UNC-3 targets are controlled in a modular manner over time ("initiation and maintenance" or "maintenance-only" modules). To describe this phenomenon, we use the term "temporal modularity in UNC-3 function" given that the function of a cell type-specific TF at a particular life stage is determined by the suite of targets it controls at that stage (**Figure 3C**). In the following

270 sections, we hone in on a single target (*cfi-1/Arid3a)* from the "maintenance-only"
271 module, aiming to dissect the molecular mechanisms underlying the temporal
272 modularity of UNC-3 function in cholinergic MNs.
273
274 **A distal enhancer is necessary for initiation and maintenance of *cfi-1/Arid3a***
275 **expression in MNs**
276 Our *cis*-regulatory analysis suggests that maintenance, but not initiation, of *cfi-1*
277 expression depends on UNC-3 (**Figure 3B**). We therefore hypothesized that the sole
278 UNC-3 binding peak on the *cfi-1* locus (located ~12 kb upstream) demarcates an
279 enhancer element selectively required for maintenance (**Figure 3B** and **4A**). If this were
280 to be the case, then it would be logical to assume that a separate *cis*-regulatory element
281 would control *cfi-1* initiation in MNs. To test this assumption, we conducted an unbiased
282 *cis*-regulatory analysis *in vivo* by generating a series of 12 transgenic reporter (GFP or
283 RFP) animals, with each reporter carrying small and contiguous DNA fragments
284 spanning a ~15 kb region (**Figure 4A**). Surprisingly, this analysis did not reveal a
285 separate initiation element. Instead, it identified a 2.5 kb distal element (reporter #7)
286 demarcated by the UNC-3 binding peak (**Figure 4A**) that drives RFP expression in
287 subsets of *unc-3*-expressing cholinergic MNs (DA, DB, VA, VB subtypes) at embryonic
288 (3-fold), larval and adult stages (**Figure 4A, C**). In addition, this 2.5 kb element also
289 showed expression at all these stages in *unc-3*-negative neurons of the nerve cord,
290 namely the GABAergic (DD, VD subtypes) MNs (**Figure 4A, C**), which will be discussed
291 later in Results. We conclude that this enhancer element is sufficient for initiation and
292 maintenance of *cfi-1* reporter expression in nerve cord MNs.
293 To test the necessity of this element, we first generated via CRISPR/Cas9 an
294 endogenous mNeonGreen (mNG) reporter allele for *cfi-1,* which also carries an auxin-
295 inducible degron (AID) tag (*mNG::AID::cfi-1*), enabling inducible depletion of CFI-1
296 (depletion experiments are described later in Results). Animals carrying the
297 *mNG::AID::cfi-1 AID* allele do not show any developmental phenotypes, suggesting that
298 the mNG::AID tag does not detectably alter *cfi-1* activity. This reporter showed
299 expression in subsets of *unc-3*-expressing MNs (DA, DB, VA, VB subtypes), GABAergic
300 nerve cord MNs (DD, VD subtypes), tail and head neurons, as well as head muscle
301 (**Figure 4A-C**), a pattern consistent with previous studies describing *cfi-1* expression
302 (Shaham and Bargmann, 2002, Kerk et al., 2017). We determined the onset of the

303 endogenous *cfi-1* reporter (*mNG::AID::cfi-1)* in MNs to be at the 3-fold embryonic stage,
304 coinciding with the onset of transgenic reporters (#7 and #8) containing the distal
305 enhancer (**Figure 4B**). Next, we employed CRISPR/Cas9 genome editing and deleted
306 769 bp that constitute the core of the UNC-3 binding peak (located ~12 kb upstream) in
307 the context of the endogenous *cfi-1* reporter (*mNG::AID::cfi-1*$^{\Delta\ enhancer\ (769\ bp)}$). We found
308 that *mNG::AID::cfi-1* expression is selectively eliminated in cholinergic (DA, DB, VA, VB)
309 and GABAergic (DD, VD) nerve cord MNs at all life stages examined (3-fold embryo,
310 L4, Day 1 adult) (**Figure 4A-B**, quantification of cholinergic MNs shown in **4D**).
311 We conclude that a distal enhancer (located ~12 kb upstream of *cfi-1*) is both
312 necessary and sufficient for *cfi-1* expression in nerve cord MNs. Genome editing
313 suggests that a 769 bp sequence within this enhancer is required for both initiation and
314 maintenance of *cfi-1* in nerve cord MNs (**Figure 4D**). In the ensuing sections, we test
315 the hypothesis that this enhancer integrates UNC-3 input for *cfi-1* maintenance in
316 cholinergic MNs, as well as UNC-3-independent input for *cfi-1* initiation in these
317 neurons.
318
319 **UNC-3 maintains *cfi-1* expression in cholinergic MNs via direct activation of the**
320 **distal enhancer**
321 The binding of UNC-3 to the distal enhancer strongly suggests UNC-3 acts directly to
322 maintain *cfi-1* expression in cholinergic MNs (**Figure 4A**). However, the UNC-3 peak is
323 spread across several hundred base pairs due to the inherently low ChIP-Seq
324 resolution; hence, the precise DNA sequences recognized by UNC-3 remained
325 unknown. Through bioinformatic analysis (see Materials and Methods), we identified 8
326 putative UNC-3 binding sites (COE motifs) within the 769 bp distal enhancer (**Figure**
327 **4E**). Using CRISPR/Cas9 technology, we simultaneously mutated all 8 motifs in the
328 context of the endogenous *cfi-1* reporter allele (*mNG::AID::cfi-1*$^{8\ COE\ motifs\ mut}$) by
329 substituting nucleotides known to be critical for DNA binding of UNC-3 orthologs
330 (Treiber et al., 2010a, Wang et al., 1993) (**Figure 4E**). During the L2 stage, expression
331 of *mNG* in MNs is not affected in *mNG::AID::cfi-1* $^{8\ COE\ motifs\ mut}$ animals, indicating early
332 *cfi-1* expression occurs normally (**Figure 4F**). Intriguingly, *mNG* expression is
333 significantly down-regulated in cholinergic MNs at later larval (L4) and adult (day 1)
334 stages, resembling the phenotype of *unc-3* null mutants (**Figure 4F**). We conclude that

335 UNC-3 binds to the distal enhancer and directly acts through one or more of these 8
336 COE motifs to maintain *cfi-1* expression in cholinergic MNs.
337 Previous studies in the nervous system have shown that a TF can maintain its
338 own expression via transcriptional activation either by itself (positive auto-regulation), or
339 in partnership with other TFs (Leyva-Diaz and Hobert, 2019, Scott et al., 2005, Xue et
340 al., 1992). We found though that *cfi-1* does not auto-regulate and UNC-3 binding at the
341 distal enhancer occurs normally in *cfi-1* null mutants (**Figure 4 – figure supplement 1**),
342 excluding a potential involvement of CFI-1 in its own maintenance.
343
344 **LIN-39 (Scr/Dfd/Hox4-5) and MAB-5 (Antp/Hox6-8) control *cfi-1* expression in**
345 **cholinergic MNs through the same distal enhancer**
346 If UNC-3 exerts a maintenance role, what are the factors that initiate *cfi-1* expression in
347 MNs? Previous work showed that two Hox proteins, LIN-39 (Scr/Dfd/Hox4-5) and MAB-
348 5 (Antp/Hox6-8), control *cfi-1* expression in MNs (Kratsios et al., 2017). However,
349 analysis was performed at the last larval stage (L4) and transgenic *cfi-1* reporter
350 animals were used. Hence, it is unclear whether LIN-39 and MAB-5 are required for
351 initiation of endogenous *cfi-1*.
352 Because *lin-39; mab-5* double null mutants are viable (Liu and Fire, 2000), we
353 performed a longitudinal analysis and found that expression of the endogenous
354 *mNG::AID::cfi-1* reporter in cholinergic MNs is severely affected at embryonic (3-fold),
355 larval (L2, L4) and adult (D1) stages (**Figure 5A-C**). Since onset of *cfi-1* expression
356 occurs at the 3-fold embryonic stage (**Figure 4B**), these results suggest LIN-39 and
357 MAB-5 are required for *cfi-1* initiation. Conversely, initiation of *cfi-1* expression is not
358 affected in a null mutant of *unc-3* (**Figure 5B-C**). Moreover, available ChIP-Seq data
359 from modENCODE (Boyle et al., 2014) indicate that LIN-39 and MAB-5 bind to the *cfi-1*
360 distal enhancer (**Figure 5A**). Expression of a 2.5 kb transgenic *cfi-1* reporter (reporter
361 #7) that carries the distal enhancer is significantly affected in *lin-39; mab-5* double
362 mutants at early larval (L2) stages (**Figure 5A, D**). These results strongly suggest that
363 LIN-39 and MAB-5 activate *cfi-1* expression directly. Although the DNA sequence of the
364 MAB-5 binding site is not known, mutation of a single, bioinformatically predicted LIN-39
365 binding site (wild-type: aaTTGAtg > mutated: aaGGGGtg) within the enhancer led to a
366 decrease in reporter gene expression at L2 (**Figure 5A, E**). This decrease was weaker
367 compared to *lin-39; mab-5* double mutants (**Figure 5C**), likely due to compensation by

368 MAB-5. Indeed, LIN-39 and MAB-5 appear to act synergistically because endogenous
369 *cfi-1* expression (*mNG::AID::cfi-1*) is mildly affected in *lin-39* single mutants, but
370 severely affected in *lin-39; mab-5* double mutants (**Figure 5F**). We conclude that the
371 Hox proteins LIN-39 and MAB-5 are necessary for *cfi-1* initiation in cholinergic MNs (left
372 panel, **Figure 5G**), and act through the same distal enhancer utilized by UNC-3 to
373 maintain *cfi-1* (right panel, **Figure 5G**).
374 If Hox proteins were only required for initiation, then endogenous *cfi-1* expression
375 should not be affected at later stages (L2, L4, D1 adults) in *lin-39; mab-5* double
376 mutants. However, this is not the case (**Figure 5B-C**), suggesting that Hox proteins play
377 an additional role at later stages. One possibility is that these proteins, like UNC-3, are
378 also required for maintenance. To test this, we used the auxin-inducible degradation
379 (AID) system and depleted the endogenous LIN-39 protein at the last larval stage (L4)
380 by using a previously described *lin-39::mNG::AID* allele (Feng et al., 2020, Zhang et al.,
381 2015). However, expression of *cfi-1* was unaffected in the adult (**Figure 5 – figure**
382 **supplement 1**). This negative result could be attributed to low and undetectable levels
383 of LIN-39 and/or functional compensation by MAB-5. We therefore used *lin-39; mab-5*
384 double (null) mutants and crossed them to *unc-3* null animals. If Hox proteins, similar to
385 UNC-3, are required for *cfi-1* maintenance in cholinergic MNs, stronger effects should
386 be present in *unc-3*; *lin-39; mab-5* triple mutants compared to *unc-3* single mutants.
387 Indeed, we found this to be the case in day 1 adult animals (graph on the right, **Figure**
388 **5C**). Supporting a maintenance role for Hox, mutation of the LIN-39 binding site within
389 the *cfi-1* enhancer (reporter #8) led to a sustained decrease in reporter gene expression
390 from L2 to adult stages (**Figure 5E**).
391 Together, our findings suggest the Hox proteins LIN-39 and MAB-5 control
392 initiation and maintenance of *cfi-1* in cholinergic MNs via the same distal *cis*-regulatory
393 region (enhancer) utilized by UNC-3 to maintain *cfi-1* (**Figure 5G**). However, this region
394 bears distinct UNC-3 and LIN-39 binding sites.
395
396 ***cfi-1/Arid3a* is required post-embryonically to maintain MN subtype identity**
397 Expression of *cfi-1* in cholinergic (DA, DB, VA, VB) MNs is maintained throughout life by
398 Hox and UNC-3 (**Figure 5G**). But why is it important to ensure continuous *cfi-1*
399 expression? Although its function in VA and VB remains unknown, CFI-1 is required
400 during early development to establish the identity of DA and DB subtypes by acting as a

401 transcriptional repressor (Kerk et al., 2017). In *cfi-1* null animals, glutamate receptor
402 subunit 4 (*glr-4/GluR),* a terminal identity gene normally activated by UNC-3 in another
403 MN subtype (SAB), becomes ectopically expressed in DA and DB neurons (**Figure 5 –**
404 **figure supplement 2**). Hence, early removal of *cfi-1* leads to DA and DB neurons
405 adopting a mixed identity. Whether CFI-1 is required post-embryonically to continuously
406 prevent DA and DB from obtaining a mixed identity is not known.
407 To enable CFI-1 protein depletion selectively at post-embryonic stages, we used
408 the *mNG::AID::cfi-1* reporter allele (**Figure 4A**), which also serves as a conditional allele
409 as it carries the auxin-inducible degron (AID) (Zhang et al., 2015). Auxin administration
410 at the first larval (L1) stage resulted in efficient depletion of *mNG::AID::cfi-1* expression,
411 which was undetectable 2 days later (**Figure 5 – figure supplement 2**). At the L3 stage
412 (2 days upon continuous auxin treatment), we observed ectopic expression of *glr-4* in
413 DA and DB neurons. These results suggest that CFI-1 is required post-embryonically to
414 prevent DA and DB neurons from adopting mixed identity, and underscore the critical
415 role of UNC-3 and Hox in maintaining *cfi-1* expression (**Figure 5G**).
416
417 **Disruption of temporal modularity in UNC-3 function leads to locomotion defects**
418 Animals carrying *unc-3* null alleles display severe locomotion defects (Feng et al.,
419 2020), likely due to combined defects in the expression of UNC-3 targets from both
420 "initiation and maintenance" and "maintenance-only" modules (**Figure 3C**). Genes from
421 the "initiation and maintenance" module include (among others) terminal identity genes
422 coding for ACh biosynthesis components (**Figure 3A**). Hence, it is conceivable that loss
423 of *unc-3* can lead to defects in ACh biosynthesis, likely contributing to locomotion
424 defects. However, it is unclear whether the expression of UNC-3 targets from the
425 "maintenance-only" module is critical for locomotion. To test this, we focused on c*fi-*
426 *1/Arid3a* and used the CRISPR-engineered allele (*mNG::AID::cfi-1* $^{8\ COE\ motifs\ mut}$) that
427 selectively affects maintenance, but not initiation, of *cfi-1* expression in cholinergic MNs
428 (**Figure 4E-F**). As controls, we used animals carrying: (**a**) the endogenous *cfi-1* reporter
429 allele (*mNG::AID::cfi-1),* (**b**) a putative null *cfi-1* allele (*ot786*) (Kerk et al., 2017), in
430 which *cfi-1* activity is affected in MNs and other neuron types of the motor circuit
431 (Pereira et al., 2015, Shaham and Bargmann, 2002), and (**c**) a deletion of the distal
432 enhancer (*mNG::AID::cfi-1*$^{\Delta enhancer(769\ bp)}$), in which both initiation and maintenance of *cfi-*
433 *1* are abrogated in nerve cord MNs (**Figure 6A**). We performed a high-resolution

434 behavioral analysis of freely moving adult (day 2) animals of the above genotypes using
435 automated multi-worm tracking technology (Javer et al., 2018b, Yemini et al., 2013). We
436 found several features related to *C. elegans* locomotion (*e.g.,* body curvature, velocity)
437 severely affected in *cfi-1 (ot786)* putative null animals (**Figure 6B-G**). Compared to *cfi-1*
438 null mutants, animals carrying the *mNG::AID::cfi-1* $^{8\ COE\ motifs\ mut}$ allele (selective
439 disruption of *cfi-1* maintenance) display milder, but statistically significant locomotion
440 defects in the adult (**Figure 6B-G**). As expected, these defects were also present in
441 animals carrying the *mNG::AID::cfi-1* $^{\Delta enhancer\ (769\ bp)}$ allele, in which both initiation and
442 maintenance of *cfi-1* expression is affected. In summary, we specifically disrupted in
443 cholinergic MNs the maintained expression of a single UNC-3 target (*cfi-1* from the
444 "maintenance-only" module) and observed locomotion defects. This analysis suggests
445 that minimal disruption of temporal modularity in UNC-3 function can affect animal
446 behavior.
447
448 **Hox proteins and UNC-3 control *bnc-1/BNC* expression in cholinergic motor**
449 **neurons**
450 Our *cis*-regulatory analysis suggested that five TFs (*cfi-1/Arid3a, bnc-1/BNC1-2, mab-*
451 *9/Tbx20, ceh-44/CUX1-2, nhr-40/nuclear hormone receptor)* require UNC-3 selectively
452 for maintenance (**Figure 3B**). An in-depth analysis of *cfi-1/Arid3a* revealed that Hox
453 proteins (LIN-39, MAB-5) and UNC-3 ensure the continuous expression of *cfi-1* in
454 subsets of *unc-3*-positive MNs (**Figure 3-5**). We next asked whether a similar
455 mechanism applies to the regulation of *bnc-1*/BNC, which is also expressed in a subset
456 of *unc-3*-positive MNs (VA, VB) and prevents them from adopting a mixed identity
457 (**Figure 5 – figure supplement 3**) (Kerk et al., 2017). Using an endogenous reporter
458 allele (*bnc-1::mNG::AID*), we found that LIN-39 and MAB-5 are required for *bnc-1*
459 expression at all stages examined (L2, L4, day 1 adult; **Figure 5 – figure supplement**
460 **3**), suggesting a role for Hox in *bnc-1* initiation and maintenance. Next, we found that
461 UNC-3 is absolutely required for *bnc-1* maintenance in the adult (day 1), albeit weaker
462 effects were also observed at L2 and L4 (**Figure 5 – figure supplement 3**). Similar to
463 *cfi-1*, these findings strongly suggest that endogenous *bnc-1* expression depends on
464 Hox and UNC-3.
465

466 **Temporal modularity of UNC-30/PITX function in GABAergic motor neurons**
467 Is temporal modularity observed in the function of other terminal selectors? To address
468 this, we focused on UNC-30/PITX, the terminal selector of GABAergic MN (DD, VD)
469 identity in the *C. elegans* nerve cord (**Figure 7A**) (Jin et al., 1994). UNC-30/PITX is
470 known to directly activate the expression of several terminal identity genes (e.g., *unc-*
471 *25*/GAD [glutamic acid decarboxylase], *unc-47*/VAGT [vesicular GABA
472 transporter])(Eastman et al., 1999), but a longitudinal analysis of target gene expression
473 in *unc-30* null animals is lacking. Using reporter strains and methodologies similar to
474 those used for UNC-3, we found that terminal identity gene (*unc-25*/GAD, *unc-*
475 *47*/VAGT) expression is affected in GABAergic MNs of *unc-30* mutants at all stages
476 examined (3-fold embryo, L2, L4, adult [day 1]) (**Figure 7B, D**), suggesting a
477 requirement for initiation and maintenance. As mentioned earlier (**Figure 4C**), *cfi-1* is
478 also expressed in GABAergic MNs (**Figure 7A**). Since UNC-3 is required for *cfi-1*
479 maintenance in cholinergic MNs, we asked whether UNC-30/PITX plays a similar role to
480 maintain *cfi-1* expression in GABAergic MNs. We found no effect at the embryonic
481 stage (3-fold), but progressively stronger effects at larval (L2, L4) and adult (day 1)
482 stages (**Figure 7C**), indicating that, in GABAergic MNs, UNC-30/PITX is selectively
483 required for the maintenance, but not initiation of *cfi-1* expression. Taken together, our
484 findings indicate that, like UNC-3 in cholinergic MNs (**Figure 3C**), the function of UNC-
485 30 in GABAergic MNs is organized into two modules (module #1: initiation and
486 maintenance; module #2: maintenance-only) (**Figure 7D-E**), suggesting temporal
487 modularity may be a shared feature among terminal selector type-TFs.
488 To gain mechanistic insights, we analyzed available UNC-30 ChIP-Seq data at
489 the L2 stage (Yu et al., 2017). UNC-30 binds to the *cis*-regulatory region of terminal
490 identity genes (*unc-25*/GAD, *unc-47*/VAGT) (**Figure 7B**), confirming previous
491 observations (Eastman et al., 1999). UNC-30 also binds to the same distal enhancer of
492 *cfi-1* in GABAergic MNs, as UNC-3 does in cholinergic MNs (**Figure 7C**). However, the
493 UNC-30 binding sites are distinct from the UNC-3 sites in this enhancer (**Figure 7C**).
494 CRISPR-mediated deletion of this enhancer abolished *cfi-1* expression in both
495 cholinergic and GABAergic MNs (**Figure 4A-B**). This finding suggests that maintenance
496 of *cfi-1* expression in two different neuron types relies on the same enhancer receiving
497 UNC-30/PITX input in GABAergic MNs and UNC-3/EBF input in cholinergic MNs.
498 Interestingly, these results provide an example of “enhancer pleiotropy” (Sabaris et al.,

499 2019), in which the same *cis*-regulatory element is used to control gene expression in
500 different neuron types.
501
502
503

504 **DISCUSSION**

505 Terminal selectors are continuously expressed TFs that determine the identity and
506 function of individual neuron types (Hobert, 2008, Hobert, 2016b). However, the breadth
507 of biological processes controlled by terminal selectors remains unclear. Moreover,
508 whether terminal selectors control an identical suite of target genes across different life
509 stages, or the suite of targets can change over time is largely unexplored. Filling such
510 knowledge gaps can help us understand how cellular identity is established during
511 development and maintained throughout life, a fundamental goal in the field of
512 developmental biology. In this study, we focus on UNC-3/Ebf, the terminal selector of
513 cholinergic MNs in the *C. elegans* nerve cord. Through ChIP-Seq, we identify in an
514 unbiased manner the direct targets of UNC-3, uncovering the breadth of biological
515 processes potentially controlled by this terminal selector. Unexpectedly, we find two
516 groups of target genes with distinct temporal requirements for UNC-3 in cholinergic
517 MNs. One group encodes different classes of proteins (e.g., receptors, transporters)
518 that require UNC-3 activation at all life stages examined. However, a second group
519 exclusively encodes MN-specific TFs that selectively require UNC-3 for maintenance of
520 their expression at late larval and adult stages. Hence, the suite of UNC-3 targets in
521 cholinergic MNs is modified across different life stages, a phenomenon we term
522 "temporal modularity" in terminal selector function. Minimal disruption of this modularity
523 by selectively removing the ability of UNC-3 to maintain expression of a single target
524 gene (the TF *cfi-1/Arid3a* from the second group) led to locomotion defects, highlighting
525 the necessity of temporal modularity for animal behavior.

526

527 **Temporal modularity in terminal selector function may represent a general**
528 **principle for neuronal subtype diversity**

529 Why is there a need for temporal modularity in the function of continuously expressed
530 TFs, such as terminal selectors? The case of UNC-3 suggests that temporal modularity
531 is necessary for generating and maintaining neuronal subtype diversity. UNC-3 is
532 continuously expressed in six MN subtypes (SAB, DA, DB, VA, VB, AS) of the *C.*
533 *elegans* ventral nerve cord (**Figure 4C**) (Pereira et al., 2015). However, most of UNC-3
534 targets from either module (modules # 1 and #2, **Figure 3C**) are expressed in some, but
535 not all, of these subtypes. By ensuring the continuous expression of genes from module
536 #1 ("initiation and maintenance" module, **Figure 3C**), such as terminal identity genes

537 [(Kratsios et al., 2012) and this study], UNC-3 consolidates the unique identity of each
538 MN subtype. However, target genes from module #2 ("maintenance-only" module,
539 **Figure 3C**) escape initiation by UNC-3, but do require UNC-3 for maintenance.
540 Interestingly, all module #2 targets code for TFs (*cfi-1/Arid3a, bnc-1/BNC1-2, mab-*
541 *9/Tbx20, ceh-44/Cux1, nhr-40*), specifically expressed in subsets of the six subtypes
542 (SAB, DA, DB, VA, VB, AS) ((Kerk et al., 2017) and this study). Three of these factors
543 (*cfi-1/Arid3a, bnc-1/Bnc1, mab-9/Tbx20)* are thought to act as transcriptional repressors
544 to prevent the adoption of mixed MN identity (Kerk et al., 2017). For example, loss of *cfi-*
545 *1* during early development results in "mixed" identity of DA and DB subtypes, as these
546 cells, in addition to their normal molecular signature, also acquire expression of genes
547 (e.g., *glr-4*/GluR) normally expressed in other MNs (**Figure 5 – figure supplement 2**).
548 Through protein depletion experiments at post-embryonic stages, we show here that
549 CFI-1 is continuously required to prevent DA and DB neurons from acquiring a mixed
550 identity. Hence, UNC-3 indirectly maintains the unique identity of individual MN
551 subtypes (DA, DB) by selectively maintaining expression of the TF *cfi-1* (from module
552 #2) during late larval and adult stages. In addition, UNC-3 acts directly to control DA
553 and DB identity by ensuring the continuous expression of *unc-129/TGFb*, a DA- and
554 DB-specific terminal identity gene (from module #1) (**Figure 3A**, **Figure 5 – figure**
555 **supplement 2**). Hence, temporal modularity in UNC-3 function can be envisioned as a
556 "double safety" mechanism for the generation and maintenance of MN diversity.
557 The mechanism of temporal modularity may represent a general paradigm of
558 how terminal selectors establish and maintain subtype identity within a class of
559 functionally related neurons. Indeed, the same terminal selector is often continuously
560 expressed in multiple subtypes of a given neuronal class (Hobert and Kratsios, 2019). In
561 mice, for example, the terminal selectors Nurr1 and Pet1 are expressed in several
562 subtypes of dopaminergic and serotonergic neurons, respectively (Kadkhodaei et al.,
563 2009, Okaty et al., 2015). However, future studies are needed to determine whether
564 temporal modularity in the function of these terminal selectors is necessary for
565 establishing and maintaining neuronal subtype identity.
566
567 **Temporal modularity offers key insights into how terminal selectors control**
568 **neuronal identity over time**
569 The prevailing hypothesis of how terminal selectors establish and maintain neuronal

570 identity is that they bind constantly, from development through adulthood, on the *cis*-
571 regulatory region of terminal identity genes, and thereby continuously activate their
572 expression (Deneris and Hobert, 2014, Hobert, 2008, Hobert and Kratsios, 2019). For
573 most terminal selectors, however, biochemical evidence for binding and longitudinal
574 analysis of terminal selector mutant animals are currently lacking. Our analysis on
575 module #1 genes (e.g., terminal identity genes) supports the aforementioned
576 hypothesis; ChIP-Seq for UNC-3 demonstrated binding on these genes (**Figure 3A, C**).
577 Moreover, our longitudinal genetic analysis together with a previous report that
578 selectively removed UNC-3 activity in adult MNs (Kerk et al., 2017) strongly suggest
579 that UNC-3 is continuously required to maintain terminal identity gene expression.
580 Interestingly, the analysis on module #2 genes provides new mechanistic insights
581 into how terminal selectors control neuronal identity over time. Instead of constantly
582 activating the same set of genes, as predicted by the above hypothesis, terminal
583 selectors can also modify the suite of their target genes at different life stages (temporal
584 modularity). This is based on the finding that UNC-3 is selectively required for
585 maintenance, not initiation, of five conserved TF-encoding genes from module #2 (*cfi-*
586 *1/Arid3a, bnc-1/BNC1-2, mab-9/Tbx20, ceh-44/Cux1, nhr-40)* (**Figure 3B-C**). Moreover,
587 by honing in on one TF (*cfi-1/Arid3a),* we identify a mechanism that enables initiation
588 and maintenance of module #2 genes (**Figure 5G**). That is, the Hox proteins LIN-39 and
589 MAB-5 control initiation of *cfi-1/Arid3a* in cholinergic MNs independently of UNC-3, but
590 *cfi-1* maintenance in these same neurons depends on both Hox and UNC-3 (**Figure**
591 **5G**). Mechanistically, we propose that Hox-dependent initiation and Hox/UNC-3-
592 dependent maintenance of *cfi-1* are "funneled" through the same distal enhancer, which
593 bears both Hox and UNC-3 binding sites. This suggests embryonic initiation and post-
594 embryonic maintenance of expression of a particular gene, in a specific cell type, can be
595 achieved by distinct TF combinations acting upon the same *cis*-regulatory region
596 (enhancer) (**Figure 5G**). This somewhat surprising mechanism differs from previous fly
597 and mouse studies reporting distinct and physically separated *cis*-regulatory regions
598 necessary for either initiation or maintenance of cell type-specific gene expression
599 (Ellmeier et al., 2002, Johnson et al., 2011, Manzanares et al., 2001, Pfeffer et al.,
600 2002, Rhee et al., 2016).
601 In summary, our findings critically extend the mechanisms underlying UNC-3
602 function. Previous work demonstrated that, in cholinergic MNs, UNC-3 not only

603 activates expression of terminal identity genes (Kratsios et al., 2012), but also prevents
604 alternative neuronal identities (Feng et al., 2020). Here, we report that the suite of UNC-
605 3 targets in these neurons can be modified at different life stages, offering key insights
606 into how terminal selectors control neuronal identity over time.
607
608 **Hox proteins collaborate with stage-specific TFs to establish and maintain MN**
609 **terminal identity**
610 During early neuronal development, Hox proteins are essential for cell survival,
611 neuronal diversity, and circuit assembly (Baek et al., 2013, Catela et al., 2016, Estacio-
612 Gomez and Diaz-Benjumea, 2014, Karlsson et al., 2010, Miguel-Aliaga and Thor, 2004,
613 Moris-Sanz et al., 2015, Philippidou and Dasen, 2013). However, their post-embryonic
614 neuronal functions remain elusive. Moreover, Hox proteins are often continuously
615 expressed in multiple cell types of a given body region (Baek et al., 2013, Hutlet et al.,
616 2016, Takahashi et al., 2004), raising the question of how do they achieve cell type-
617 specificity in their function. Our findings on mid-body Hox proteins LIN-39 and MAB-5
618 begin to address this question.
619 LIN-39 and MAB-5 are continuously expressed in multiple cell types located at the
620 *C. elegans* mid-body region (Clark et al., 1993, Cowing and Kenyon, 1992, Feng et al.,
621 2020, Maloof and Kenyon, 1998). We find that LIN-39 and MAB-5 exert a cell type-
622 specific function; they are required to initiate (in embryo) and maintain (post-
623 embryonically) *cfi-1* expression in specific subsets of cholinergic MNs (DA, DB, VA, VB;
624 **Figure 4C**). Such specificity likely arises through collaboration with distinct TFs
625 responsible for either initiation or maintenance of *cfi-1* (**Figure 5G**). Supporting this
626 scenario, Hox (LIN-39, MAB-5) and UNC-3 are co-expressed in DA, DB, VA, and VB
627 neurons (Feng et al., 2020). Moreover, UNC-3 is selectively required for *cfi-1*
628 maintenance (not initiation) in these neurons (**Figure 5G**). We surmise that other, yet-
629 to-be-identified factors collaborate with Hox proteins at early stages to initiate *cfi-1*
630 expression specifically in DA, DB, VA, and VB neurons. Such initiation-specific factors
631 likely act through the same distal enhancer because its deletion completely abolished
632 *cfi-1* expression in these neurons at early (and late) stages (**Figure 4D, 5G**). In
633 summary, we propose that Hox proteins collaborate with distinct TFs over time, that is,
634 initiation-specific factors and the terminal selector UNC-3, to ensure continuous
635 expression of *cfi-1/Arid3a* in specific subtypes of cholinergic MNs. This mechanism may

636 extend to the regulation of terminal identity genes, as we previously showed that LIN-39
637 and UNC-3 are required to maintain expression of *acr-2/* human CHRNA1
638 (acetylcholine receptor subunit) and *unc-77/* human NALCN (sodium channel) in
639 cholinergic MNs (Feng et al., 2020). Altogether, these findings offer mechanistic insights
640 into the recently proposed hypothesis that Hox proteins in *C. elegans* collaborate with
641 terminal selectors to establish and maintain neuronal terminal identity (Kratsios et al.,
642 2017, Zheng et al., 2015).
643
644 **Limitations of this study**
645 By conducting a longitudinal analysis for 14 UNC-3 target genes, we identified two
646 groups with distinct temporal requirements (modules #1 and #2 in **Figure 3C**). It is likely
647 though that UNC-3 temporally controls other targets though additional modules. For
648 example, animals lacking *unc-3* display severe axon guidance defects in cholinergic
649 MNs (Prasad et al., 1998), but the underlying mechanisms remain unknown. Since axon
650 guidance molecules are often expressed in a transient fashion during early neuronal
651 development, we speculate that UNC-3 may transiently activate expression of such
652 molecules, a possibility that would add another temporal module in UNC-3 function.
653 In addition, the breadth of biological processes controlled by terminal selectors
654 remains largely unknown. Our ChIP-Seq analysis potentially implicates UNC-3 in a
655 range of biological processes. First, this dataset significantly extends previous reports
656 on the role of UNC-3 in neuronal terminal identity (Kim et al., 2005, Kratsios et al., 2012)
657 by identifying hundreds of terminal identity genes (42.18% of total ChIP-Seq hits) as
658 putative UNC-3 targets. Second, the ChIP-Seq dataset suggests new roles for UNC-3 in
659 neuronal metabolic pathways (24.14% of UNC-3 target genes code for enzymes) and
660 gene regulatory networks (24.07% of UNC-3 targets are TFs and nucleic acid-binding
661 proteins). However, future RNA-Sequencing studies in *unc-3*-depleted MNs are
662 necessary to correlate gene expression changes with UNC-3 ChIP-Seq data, and
663 thereby identify *bona fide* targets and biological processes under UNC-3 control.
664
665 **Temporal modularity may be a shared feature among continuously expressed TFs**
666 This study suggests that the suite of targets of two *C. elegans* terminal selectors (UNC-
667 3/Ebf and UNC-30/Pitx) can be modified over time, providing evidence for temporal
668 modularity in their function. Given that terminal selectors, as well as other neuron type-

669 specific TFs with continuous expression, have been described in both invertebrate and
670 vertebrate species (Deneris and Hobert, 2014, Hobert and Kratsios, 2019, Mayer et al.,
671 2018, Mi et al., 2018), it will be interesting to determine the potential generality of the
672 temporal mechanism described here. Supporting this possibility, the terminal selector of
673 serotonergic neurons in mice (Pet-1) activates expression of serotonin biosynthesis
674 proteins during development, but appears to switch transcriptional targets at later life
675 stages (Wyler et al., 2016). Outside the nervous system, cell type-specific TFs with
676 continuous expression have been described in worms, flies and mice (Pikkarainen et
677 al., 2004, Soler et al., 2012, Wiesenfahrt et al., 2016, Zhou et al., 2017). Future studies
678 will determine whether the principle of temporal modularity is widely employed for the
679 control of cell type identity.
680
681
682

683 **MATERIALS AND METHODS**

684

685 ***C. elegans* strain culture**

686 Worms were grown at 20˚C or 25˚C on nematode growth media (NGM) plates supplied
687 with *E. coli* OP50 as food source (Brenner, 1974). A list of all *C. elegans* strains used is
688 provided in **Supplementary file 4**.

689

690 **Generation of transgenic animals carrying transcriptional fusion reporters**

691 Reporter gene fusions for *cis*-regulatory analyses and validation of newly identified
692 UNC-3 target genes were made with PCR fusion (Hobert, 2002). Genomic regions were
693 amplified and fused to the coding sequence of *tagrfp* followed by the *unc-54* 3' UTR. To
694 mutate the LIN-39 binding motif, the reporter fusion was first introduced into the pCR-
695 XL-TOPO vector using the TOPO XL PCR cloning kit (Invitrogen). Then, mutagenesis
696 PCR was performed, and single clones containing plasmids that carry the desired
697 mutation were isolated. PCR fusion DNA fragments were injected into young adult *pha-*
698 *1(e2123)* hermaphrodites at 50 ng/µl together with *pha-1* (pBX plasmid) as co-injection
699 marker (50 ng/µl).

700

701 **Chromatin Immunoprecipitation (ChIP)**

702 ChIP assay was performed as previously described (Yu et al. 2017; Zhong et al. 2010)
703 with the following modifications. Synchronized L1 *unc-3 (ot839[unc-3::gfp])* worms and
704 N2 worms were cultured on 10 cm plates seeded with OP50 at 20°C overnight. Late L2
705 worms were cross-linked and resuspended in FA buffer supplemented with protease
706 inhibitors (150 mM NaCl, 10 µl 0.1 M PMSF, 100 µl 10% SDS, 500 µl 20% N-Lauroyl
707 sarsosine sodium, 2 tablets of cOmplete ULTRA Protease Inhibitor Cocktail [Roche
708 Cat.# 05892970001] in 10ml FA buffer). For each IP experiment, 200 µl worm pellet was
709 collected. The sample was then sonicated using a Covaris S220 at the following
710 settings: 200 W Peak Incident Power, 20% Duty Factor, 200 Cycles per Burst for 1 min.
711 Samples were transferred to centrifuge tubes and spun at the highest speed for 15 min.
712 The supernatant was transferred to a new tube, and 5% of the material was saved as
713 input and stored at -20°C. The remainder was incubated with 2 µl GFP antibody (Abcam
714 Cat.# ab290) at 4°C overnight. Wild-type (N2) worms do not carry the GFP tag and
715 serve as negative control. The *unc-3 (ot839[unc-3::gfp])* CRIPSR generated allele was

716 used in order to immunoprecipitate the endogenous UNC-3 protein. On the next day, 20
717 ul Dynabeads Protein G (1004D) was added to the immunocomplex, which was then
718 incubated for 2 hr at 4°C. The beads then were washed at 4°C twice with 150 mM NaCl
719 FA buffer (5 min each), and once with 1M NaCl FA buffer (5 min). The beads were
720 transferred to a new centrifuge tube and washed twice with 500 mM NaCl FA buffer (10
721 min each), once with TEL buffer (0.25 M LiCl, 1% NP-40, 1% sodium deoxycholate,
722 1mM EDTA, 10 mM Tris-HCl, pH 8.0) for 10 min, and twice with TE buffer (5 min each).
723 The immunocomplex was then eluted in 200 µl elution buffer (1% SDS in TE with 250
724 mM NaCl) by incubating at 65°C for 20 min. The saved input samples were thawed and
725 treated with the ChIP samples as follows. One (1) µl of 20 mg/ml proteinase K was
726 added to each sample and the samples were incubated at 55°C for 2 hours then 65°C
727 overnight (12-20 hours) to reverse cross-link. The immonuprecipitated DNA was purified
728 with Ampure XP beads (A63881) according to manufacturer's instructions.
729
730 **ChIP-sequencing data analysis**
731 Unique reads were mapped to the *C. elegans* genome (ce10) with bowtie2 (Langmead
732 and Salzberg, 2012). Peak calling was then performed with MACS2 (minimum q-value
733 cutoff for peak detection: 0.005). For visualization purposes, the sequencing depth was
734 normalized to 1x genome coverage using bamCoverage provided by deepTools
735 (Ramirez et al., 2016), and peak signals were shown in IGV. Heatmap of peak coverage
736 in regard to UNC-3 enrichment center was generated with NGSplot (Shen et al., 2014).
737 The average profile of peaks binding to TSS region was generated with ChIPseeker (Yu
738 et al., 2015). To study the distribution of peaks genome-wide, the peaks were annotated
739 using annotatePeaks.pl provided by Homer (Heinz et al., 2010), and each peak was
740 assigned to a gene with the nearest TSS. For *de novo* motif discovery, sequences
741 containing 100bp around the centers of each peak (from -50bp to +50bp) were
742 extracted and supplied to findMotifsGenome.pl provided by Homer.
743
744 **Protein Class Ontology analysis using PANTHER**
745 Protein Class Ontology analysis was performed on 1,478 UNC-3-bound genes out of
746 the 3,502 protein-coding genes. The number of genes is significantly lower than the
747 number of peaks because Panther analysis only considers genes with known protein
748 class terms.

749

750 **Targeted genome editing**

751 The *cfi-1* endogenous reporter strain *kas16 [mNG::AID::cfi-1]* was generated by
752 employing CRISPR/Cas9 genome editing and inserting
753 the *mNG::3xFLAG::AID* cassette immediately after the ATG of *cfi-1*. The *cfi-1* enhancer
754 knock-out allele *mNG::AID::cfi-1*$^{\Delta enhancer\ (769\ bp)}$ was generated by using two guide RNAs
755 flanking the *cfi-1* enhancer to guide excision of the genomic region, which was then
756 followed by homology dependent repair (HDR) to create a 769 bp deletion (-11,329 bp
757 to -12,097 bp). The UNC-3 binding motif mutation allele *mNG::AID::cfi-1*$^{8\ COE\ motifs\ mut}$
758 was generated by creating nucleotide substitutions in the repair template, which
759 carries homology arms complementary to the *cfi-1* enhancer region and is then
760 introduced into the genome through HDR.

761

762 **Microscopy**

763 Imaging slides were prepared by anesthetizing worms with sodium azide (NaN_3, 100
764 mM) and mounting them on a 4% agarose pad on glass slides. Images were taken with
765 an automated fluorescence microscope (Zeiss, Axio Imager Z2). Images containing
766 several z stacks (0.50 µm intervals between stacks) were taken with Zeiss Axiocam 503
767 mono using the ZEN software (Version 2.3.69.1000, Blue edition). Representative
768 images are shown following max-projection of 2-5 µm Z-stacks using the maximum
769 intensity projection type. Image reconstruction was performed with Image J (Schindelin
770 et al., 2012).

771

772 **Motor neuron subtype identification**

773 The identification of specific MN subtypes expressing a given UNC-3 target gene was
774 assessed based on the following: (a) co-localization with fluorescent reporters that label
775 specific MN subtypes; (b) Invariant position of neuronal cell bodies along the ventral
776 nerve cord; (c) Birth order of specific motor neuron subtypes (e.g. during
777 embryogenesis or post-embryogenesis); (d) Total cell numbers in each motor neuron
778 subtype.

779

780 **Bioinformatic prediction of binding motifs**

781 Information of the LIN-39 binding motif is curated in the Catalog of Inferred Sequence
782 Binding Preferences database (http://cisbp.ccbr.utoronto.ca). To predict and identify
783 LIN-39 binding motifs and UNC-3 binding motifs (identified in this paper) in the *cfi-1*
784 enhancer (-11,391 bp to -12,146 bp), we utilized tools provided by MEME (Multiple
785 Expectation maximization for Motif Elicitation) bioinformatics suite (http://meme-
786 suite.org/), and performed FIMO (Find Individual Motif Occurrences) motif scanning
787 analysis.
788
789 **Temporally controlled protein degradation**
790 Temporally controlled protein degradation was achieved with the auxin-inducible
791 degradation system (Zhang et al., 2015). TIR1 expression was driven by the
792 ubiquitously active *eft-3* promoter in the transgene *ieSi57 [eft-3prom::tir1]* or a
793 transgene that drives TIR1 selectively in neurons (*otTi28*). To induce degradation of
794 LIN-39 and CFI-1 proteins, the following alleles were used: *lin-39 (kas9 [lin-*
795 *39::mNG::AID]), and cfi-1 (kas16 [mNG::AID::cfi-1]).* L1 or L4 worms were grown at 20
796 ˚C on NGM plates coated with 4 nM auxin (indole-3-acetic acid [IAA] dissolved in
797 ethanol) or ethanol (negative control) for 1 day or 4 days before tested (see figure
798 legends for more details). All plates were shielded from light.
799
800 **Worm tracking**
801 Worms were maintained as mixed stage populations by chunking on NGM plates with
802 *E. coli* OP50 as the food source. Worms were bleached and the eggs were allowed to
803 hatch in M9 buffer to arrest as L1 larvae. L1 larvae were refed on OP50 and allowed to
804 grow to day 2 or adulthood. On the day of tracking, five worms were picked from the
805 incubated plates to each of the imaging plates (see below) and allowed to habituate for
806 30 minutes before recording for 15 minutes. Imaging plates are 35 mm plates with 3.5
807 mL of low-peptone (0.013% Difco Bacto) NGM agar (2% Bio/Agar, BioGene) to limit
808 bacteria growth. Plates are stored at 4°C for at least two days before use. Imaging
809 plates are seeded with 50µl of a 1:10 dilution of OP50 in M9 the day before tracking and
810 left to dry overnight with the lid on at room temperature.
811
812 **Behavioral feature extraction and analysis**

All videos were analyzed using Tierpsy Tracker to extract each worm's position and posture over time (Javer et al., 2018a). These postural data were then converted into a set of behavioral features selected from a large set of features as previously described (Javer et al., 2018b). For each strain comparison, we performed unpaired two-sample t-tests independently for each feature. The false discovery rate was controlled at 5% across all strain and feature comparisons using the Benjamini Yekutieli procedure.

Statistical analysis

For data quantification, graphs show values expressed as mean ± standard error mean (SEM) of animals. The statistical analyses were performed using the unpaired t-test (two-tailed). Calculations were performed using the GraphPad QuickCalcs online software (http://www.graph- pad.com/quickcalcs/). Differences with $p<0.05$ were considered significant.

Data accessibility

The accession number for the UNC-3 ChIP-seq data is GEO: GSE143165

ACKNOWLEDGEMENTS

We thank the *Caenorhabditis* Genetics Center (CGC), which is funded by NIH Office of Research Infrastructure Programs (P40 OD010440), for providing strains. We thank the lab of Oliver Hobert for providing the OH14930 strain and Kaiyuan Tang for generating reporter gene constructs. We are grateful to Edwin Ferguson, Oliver Hobert, Daniele Canzio, Catarina Catela, and Weidong Feng for comments on this manuscript. This work was supported by a training grant [University of Chicago Initiative for Maximizing Student Development (IMSD), 2R25GM109439-06] to A.O, a training grant (T32 GM007183) to E. C., a Whitehall Foundation grant to P.K., grants from National Institute of Neurological Disorders and Stroke (NINDS) of the NIH (Award Numbers R00NS084988 and R21NS108505) to P.K., and a Medical Research Council grant MC-A658-5TY30 to A.E.X.B.

AUTHOR CONTRIBUTIONS

Y. L., Data curation, Investigation, Visualization, Methodology, Writing—original draft, review and editing; A.O., E. C., Formal analysis, Validation, Investigation; M.O., P. D., O. G., J. A., P.I., Investigation; A.E.X.B., Project administration, Writing—editing; P. K., Conceptualization, Supervision, Investigation, Funding acquisition, Project administration, Writing— original draft, review and editing.

DECLARATION OF INTERESTS

The authors declare no competing interests.

855 **LEGENDS OF FIGURES AND TABLES**

856 **Figure 1. Mapping UNC-3 binding genome-wide with ChIP-Seq.**

857 **A:** Diagram illustrating the endogenous reporter allele of UNC-3. GFP is inserted
858 immediately upstream of *unc-3*'s stop codon. Below, a representative image at L2 stage
859 showing expression of UNC-3::GFP fusion protein in cholinergic MN nuclei. Region
860 highlighted in dashed box is enlarged. Scale bar, 20 μm.

861 **B:** Quantification of terminal identity gene markers that report expression of known
862 UNC-3 targets (*cho-1/ChT, unc-17/VAChT, ace-2/AChE*) in WT and *ot839 [unc-3::gfp]*
863 animals at the L4 stage (N = 15). N. S.: not significant.

864 **C:** Heatmap of UNC-3 ChIP-Seq signal around 1.0 kb of the center of the binding peak.

865 **D:** Summary plot of UNC-3 ChIP-Seq signal with a 95% confidence interval (grey area)
866 around 3.0 kb of the TSS. The average signal peak is detected at ~200 bp upstream of
867 the TSS.

868 **E:** *de novo* motif discovery analysis of 6,892 UNC-3 binding peaks identifies a 12 bp-
869 long UNC-3 binding motif.

870 **F:** Pie chart summarizes genomic distribution of UNC-3 ChIP-Seq signal.

871

872 **Figure 2. Global analyses of UNC-3 ChIP-Seq data.**

873 **A:** Snapshots of UNC-3 ChIP-Seq and input (negative control) signals at the *cis*-
874 regulatory regions of known UNC-3 targets (*cho-1/ChT, unc-17/VAChT, acr-2/AChR,*
875 *glr-4/GluR*).

876 **B:** Graph summarizing protein class ontology analysis of putative target genes of UNC-
877 3 identified by ChIP-Seq. Out of the 3,502 protein-coding UNC-3 targets, 1,425 encode
878 for proteins with known protein class terms and these were the ones considered by
879 PANTHER. This analysis classifies UNC-3 targets into 3 broad categories: terminal
880 identity genes, gene expression regulators, and enzymes.

881 **C:** Pie chart breaking down TF families that show UNC-3 binding.

882

883 **Figure 3. Terminal identity genes and transcription factors display distinct**
884 **temporal requirements for UNC-3.**

885 **A:** Top: snapshots of UNC-3 ChIP-Seq and input (negative control) signals at the *cis*-
886 regulatory regions of 4 cholinergic terminal identity genes (*acr-2/AChR, unc-129/TFGb,*
887 *glr-4/GluR,* and *unc-17/VAChT*). The length of DNA elements included in each reporter

888 is shown. Bottom: quantification of terminal identity gene reporters in WT and *unc-3*
889 *(n3435)* animals at 3 different developmental stages – L2, L4, and day 1 adults (N ⩾
890 12). UNC-3 is required for both initiation and maintenance of all 4 terminal identity
891 genes. *** $p < 0.001$.
892 **B:** Top: snapshots of UNC-3 ChIP-Seq and input (negative control) signals at the *cis*-
893 regulatory regions of 5 transcription factors (*cfi-1/Arid3a, bnc-1/Bnc1, nhr-40, mab-*
894 *9/Tbx20, and ceh-44/Cux1*). The length of DNA elements included in each reporter is
895 shown. Middle: representative images of WT L4 animals showing expression of the
896 transgenic reporters in MNs. Scale bar, 20 μm. Bottom: quantification of transcription
897 factor reporters in WT and *unc-3 (n3435)* animals at 3 different developmental stages –
898 L2, L4, and young adults (day 1 or day 3) (N ⩾ 12). UNC-3 is required for maintenance,
899 but not initiation of the 5 TFs. N.S.: not significant, * $p < 0.05$, *** $p < 0.001$.
900 **C:** Schematic summarizing the phenomenon of temporal modularity in UNC-3 function.
901 The first module consists of terminal identity genes and TFs (**Figure S2**), which require
902 UNC-3 for both initiation and maintenance of gene expression. The second module
903 consists exclusively of TFs that require UNC-3 only for maintenance.
904
905 **Figure 4. UNC-3 acts through a distal enhancer to maintain *cfi-1* expression in**
906 **cholinergic motor neurons.**
907 **A:** Top: Snapshots of UNC-3 ChIP-Seq and input (negative control) signals at the *cis*-
908 regulatory region of *cfi-1*. The grey bar highlights an UNC-3 binding peak located ~12 kb
909 upstream of the TSS of *cfi-1* (-11,391 bp to -12,146 bp). Bottom: schematic showing the
910 strategy of constructing *cfi-1* reporters. Twelve transcriptional fusion reporters ([-1 bp to
911 -8,170 bp], #2 [993 bp to 3,764 bp], #3 [547 bp to -1,173 bp], #4 [-1,164 bp to -2,875
912 bp], #5 [-2,865 bp to -6,141 bp], #6 [-8,162 bp to -11,346 bp], #7 [-11,329 bp to -13,824
913 bp], #8 [-11,329 bp to -11,881 bp], #9 [-11,851 bp to -12,234 bp], #10 [-12,223 bp to -
914 12,722 bp], #11 [-12,705 bp to -13,284 bp], and #12 [-13,263 bp to -13,824 bp]) carry
915 *cis*-regulatory regions fused to fluorescent reporters (GFP or RFP). The endogenous
916 reporter alleles (*mNG::AID::cfi-1* and *mNG::AID::cfi-1* $^{\Delta enhancer\ (769\ bp)}$) have an in-frame
917 fluorescent protein mNeonGreen (mNG) insertion immediately after the ATG of *cfi-1*.
918 The enhancer KO allele *mNG::AID::cfi-1* $^{\Delta enhancer\ (769\ bp)}$ carries a 769 bp deletion (-
919 11,329 bp to -12,097 bp). Table on the right summarizes the expression pattern of each
920 reporter allele at L4 stage. N ⩾ 12. +: reporter expressed, –: reporter not expressed,

921 +/–: reporter partially expressed in the respective neurons. Number of independent
922 transgenic lines tested for each reporter is shown on the right.
923 **B:** Representative images showing the expression of reporter #7, reporter #8,
924 *mNG::AID::cfi-1*, and *mNG::AID::cfi-1* $^{\Delta enhancer\ (769\ bp)}$ at specific life stages. Areas
925 highlighted in dashed boxes are enlarged and presented on the right side of each
926 picture. The onset of *cfi-1* expression occurs at the 3-fold embryonic stage. mNG+ MNs
927 are annotated with arrowheads. Scale bars, 5 μm (3-fold embryos); 20 μm (larvae and
928 adults).
929 **C:** Schematic summarizing the expression pattern of *cfi-1* and *unc-3* in nerve cord MNs.
930 **D:** Quantification of the number of cholinergic MNs expressing endogenous *cfi-1*
931 (*mNG::AID::cfi-1)* in WT and animals carrying the enhancer deletion (*mNG::AID::cfi-1*
932 $^{\Delta enhancer\ (769\ bp)}$). Deletion of the enhancer element located ~12 kb upstream of the TSS of
933 *cfi-1* completely abolishes *cfi-1* expression in MNs at all tested stages. A red fluorescent
934 marker (*ttr-39::mCherry*) for GABAergic MNs was used to exclude these neurons from
935 the quantification. Cholinergic MNs expressing *cfi-1* were positive for mNG and negative
936 for mCherry.
937 **E:** Bioinformatic analysis predicted 8 UNC-3 binding sites (COE motifs, shown as pink
938 boxes) in the *cfi-1* enhancer region, which displays UNC-3 binding (-11,391 bp to -
939 12,146 bp). Using CRISPR/Cas9, these 8 motifs were mutated by substituting duplets
940 or triplets of nucleotides as shown below, thereby generating the strain *cfi-1 (syb1856*
941 *[mNG::AID::cfi-1*$^{8\ COE\ motifs\ mut}$]).
942 **F:** Quantification of the number of cholinergic MNs expressing the endogenous *cfi-1*
943 reporter (*mNG::AID::cfi-1)* in WT and *unc-3 (n3435)* animals, as well as in animals with
944 mutated COE motifs (*mNG::AID::cfi-1*$^{8\ COE\ motifs\ mut}$) at L2, L4, and day 1 adult stages (N
945 $\geqslant$ 12). N.S.: not significant, *** $p < 0.001$.
946
947 **Figure 5. UNC-3 and Hox control *cfi-1* expression in cholinergic MNs.**
948 **A:** A snapshot of UNC-3 (L2 stage), LIN-39 (L3 stage), and MAB-5 (L2 stage) ChIP-Seq
949 signals at the *cfi-1* locus. UNC-3, LIN-39, and MAB-5 bind to the same *cfi-1* enhancer
950 (highlighted in gray). Below: Schematics illustrating the reporters used in the rest of the
951 figure.
952 **B:** Representative images showing the expression of the *mNG::AID::cfi-1* in WT, *unc-3*
953 *(n3435)*, and *lin-39 (n1760); mab-5 (e1239)* animals during 3-fold embryonic, L2, L4,

954 and day 1 adult stages. *cfi-1* is expressed in 4 cholinergic MN subtypes (DA, DB, VA,
955 and VB). DA and DB are born embryonically, while VA and VB are born post-
956 embryonically. Areas highlighted in dashed boxes are enlarged and presented on the
957 right side of each picture. mNG+ MNs are annotated with arrowheads. Scale bars, 5 μm
958 (3-fold embryos); 20 μm (larvae and adults).
959 **C:** Quantification of the number of cholinergic MNs expressing the endogenous *cfi-1*
960 reporter (*mNG::AID::cfi-1)* in WT animals, *unc-3 (n3435)* mutants, *lin-39 (n1760); mab-5*
961 *(e1239)* double mutants, and *unc-3 (n3435); lin-39 (n1760); mab-5 (e1239)* triple
962 mutants during 3-fold embryonic, L2, L4, and day 1 adult stages ($N \geqslant 12$). N.S.: not
963 significant, *** $p < 0.001$. A red fluorescent marker (*ttr-39::mCherry*) for GABAergic MNs
964 was used to exclude these neurons from the quantification. Cholinergic MNs expressing
965 *cfi-1* were positive for mNG and negative for mCherry.
966 **D:** Quantification of the expression of transgenic *cfi-1* reporter #7 in WT and *lin-39*
967 *(n1760); mab-5 (e1239)* animals at L2 stage ($N = 13$). Reporter expression is strongly
968 affected in *lin-39 (-); mab-5 (-)* double mutants. *** $p < 0.001$.
969 **E:** Quantification of the WT transgenic reporter #8 and the same reporter with the LIN-
970 39 binding site mutated (point mutations) at larval (L2) and adult (D3) stages ($N \geqslant 13$). *
971 $p < 0.05$.
972 **F:** Quantification of the expression of the *mNG::AID::cfi-1* allele in WT animals, *lin-39*
973 *(n1760)* single mutants, and *lin-39 (n1760); mab-5 (e1239)* double mutants at the L2
974 stage ($N \geqslant 12$). While the number of cholinergic MNs with *cfi-1* expression is mildly
975 decreased in *lin-39* single mutants, more severe effects are observed in double
976 mutants. *** $p < 0.001$.
977 **G:** Schematic summarizing the mechanisms underlying initiation and maintenance of
978 *cfi-1* expression in cholinergic MNs.
979
980 **Figure 6. Disruption of temporal modularity in UNC-3 function leads to**
981 **locomotion defects**
982 **A:** Schematics illustrating four *cfi-1* alleles tested for behavioral analysis.
983 **B-G:** Examples of six locomotion features significantly disrupted in animals carrying a
984 putative null *(ot786)* allele for *cfi-1*. Locomotion analysis was performed on day 2 adult
985 worms. Animals lacking *cfi-1* expression (initiation and maintenance) specifically in MNs
986 (*mNG::AID::cfi-1* $^{\Delta enhancer\ (769\ bp)}$) and animals unable to maintain *cfi-1* expression in

987 cholinergic MNs (*mNG::AID::cfi-1*$^{8\ COE\ motifs\ mut}$) display locomotion defects when
988 compared to control *mNG::AID::cfi-1* animals. As expected, these defects are milder
989 when compared to animals carrying the *cfi-1* (*ot786*) allele. Panels B-F show locomotion
990 features related to body curvature, whereas panel G shows radial velocity of the neck. A
991 detailed description of each locomotion feature is provided below:
992 (**B**) curvature_std_midbody_w_backward_abs_10th: 10th percentile of the absolute
993 value of the standard deviation of the curvature of the midbody, while worm is moving
994 backwards.
995 (**C**) curvature_tail_w_backward_abs_90th: 90th percentile of the absolute value of the
996 curvature of the tail, while worm is moving backwards.
997 (**D**) curvature_std_midbody_w_backward_50th: 50th percentile of the standard deviation
998 of the curvature of the midbody, while worm is moving backwards.
999 (**E**) curvature_std_hips_abs_10th: 10th percentile of the absolute value of the standard
1000 deviation of the curvature of the hips.
1001 (**F**) curvature_std_hips_abs_50th: 50th percentile of the absolute value of the standard
1002 deviation of the curvature of the hips
1003 (**G**) d_rel_to_body_radial_vel_neck_w_forward_90th: 90th percentile of the derivative of
1004 radial velocity of the neck relative to the centroid of the midbody points, while worm is
1005 moving forwards.
1006
1007
1008 **Figure 7. Temporal modularity in UNC-30/Pitx function in GABAergic MNs.**
1009 **A:** Schematic summarizing the expression of *cfi-1/Arid3a, unc-3/Ebf, unc-30/Pitx, unc-*
1010 *25/GAD,* and *unc-47/VGAT* in MN subtypes of the *C. elegans* ventral nerve cord.
1011 **B:** Schematic showing time of birth and cell body position of GABAergic nerve cord
1012 MNs. DD neurons are born embryonically. VD neurons are born post-embryonically.
1013 **C:** Bioinformatic analyses predict 4 UNC-30 binding sites (yellow boxes) in the *cfi-1*
1014 enhancer. The location of UNC-3 and LIN-39 binding sites are also shown.
1015 **D:** Top: snapshots of UNC-30 ChIP-Seq and input (negative control) signals at the *cis-*
1016 regulatory regions of 2 GABAergic terminal identity genes (*unc-25/GAD, unc-47/VGAT*).
1017 Bottom: quantification of the expression of transgenic reporters in WT and *unc-30*
1018 *(e191)* animals at 4 different developmental stages – 3-fold embryo, L2, L4, and day 1

1019 adults (N = 15). UNC-30 is required for both initiation and maintenance of *unc-25/GAD*
1020 and *unc-47/VGAT*. *** p < 0.001.
1021 **E:** Top: a snapshot of UNC-3 ChIP-Seq and UNC-30 ChIP-Seq signals at the *cfi-1*
1022 locus. Bottom: quantification of the number of MNs expressing the endogenous reporter
1023 *mNG::AID::cfi-1* in WT and *unc-30 (e191)* animals. All *cfi-1*-expressing MNs in the
1024 ventral cord (cholinergic and GABAergic MNs) were counted in 3-fold embryos due to a
1025 lack of a specific marker that labels GABAergic MNs in embryos. Expression of *cfi-1*
1026 specifically in GABA neurons was quantified at L2, L4, and day 1 adult stages (N ⩾ 12).
1027 At those stages, cholinergic MNs were identified based on a fluorescent marker (*cho-*
1028 *1::mChOpti*), which are ruled out during scoring. GABAergic MNs were scored positive
1029 for *cfi-1* expression when the *mNG::AID::cfi-1* (green) expression co-localized with *ttr-*
1030 *39::mCherry* (red). N.S.: not significant, *** p < 0.001.
1031
1032
1033 **Table 1: A summary of the *cis*-regulatory analysis to identify novel transcription**
1034 **factors controlled by UNC-3**. Reporter alleles of each TF were built and examined for
1035 expression pattern. TFs that are expressed in MNs were further tested for UNC-3
1036 dependency. Ten of 16 tested TFs (62.5%) show expression in MNs, of which 9 require
1037 UNC-3 activity for normal expression. Two reporters were generated for *nhr-1* and *nhr-*
1038 *40* because two distinct UNC-3 ChIP-Seq peaks were found in the *cis*-regulatory region
1039 of these genes. N/A: Not applicable.
1040

1041 **LEGENDS OF SUPPLEMENTARY FIGURES**

1042 **Figure 1 – figure supplement 1. UNC-3 ChIP-Seq results yield genome-wide**
1043 **enrichment of UNC-3.**

1044 **A:** Fingerprint plot indicating localized, strong enrichment of UNC-3 in the genome.
1045 Specifically, when counting the reads contained in 93% of all genomic bins (data point
1046 0.93, 0.5 on UNC-3 ChIP curve), only 50% of the maximum number of reads are
1047 reached, which indicates 7% of the genome contains half of total sequencing reads from
1048 the ChIP sample.

1049 **B:** Snapshots of UNC-3 ChIP-Seq and input (negative control) signals at the *cis*-
1050 regulatory regions of known UNC-3 targets (*del-1, acc-4, twk-13, dbl-1, unc-77,* and
1051 *twk-40*).

1052

1053 **Figure 3 – figure supplement 1. UNC-3 directly controls the expression of several**
1054 **TF reporters in MNs.**

1055 **A-C:** Top: snapshots of UNC-3 ChIP-Seq and input (negative control) signal at the *cis*-
1056 regulatory regions of 5 TF-encoding gens (*nhr-1, ztf-26, zfh-2, nhr-49, nhr-19*).
1057 Transgenic RFP reporters contain the *cis*-regulatory regions bound by UNC-3, as well
1058 as flanking sequences. Middle: representative images of WT L4 animals showing
1059 expression of the transgenic reporters in nerve cord MNs. Scale bar, 20 μm. Bottom:
1060 quantification of TF reporters in WT and *unc-3 (n3435)* animals at 3 different
1061 developmental stages – L2, L4, and day 3 adult. *nhr-1, ztf-26,* and *zfh-2* are activated
1062 by UNC-3 **(A)**, while *nhr-49* is repressed by UNC-3 **(B)** and *nhr-19* does not appear to
1063 be controlled by UNC-3 **(C)**. N $\geqslant$ 15. N.S.: not significant, * $p < 0.05$, ** $p < 0.01$, *** $p <$
1064 0.001.

1065 **D:** Three TF reporters (*ccch-3, ztf-17, nhr-1*) are not expressed in nerve cord MNs, but
1066 show expression in head neurons. Top: snapshots of UNC-3 ChIP-seq and input
1067 (negative control) signals at the *cis*-regulatory regions of *ccch-3, ztf-17,* and *nhr-1*.
1068 Transgenic RFP reporters contain the *cis*-regulatory regions bound by UNC-3. Bottom:
1069 representative images of WT L4 animals showing expression of the transgenic reporters
1070 in some unidentified neurons of the head. It is known that UNC-3 is expressed in some
1071 head neurons.

1072

1073

1074 **Figure 4 – figure supplement 1: CFI-1 does not auto-regulate.**
1075 **A:** Snapshots of UNC-3 ChIP-seq signal at the *cfi-1* locus in WT and *cfi-1 (ot786)*
1076 animals. UNC-3 binds to the *cfi-1* enhancer normally in *cfi-1 (ot786)* mutants.
1077 **B:** Quantification of the number of MNs expressing the transcriptional fusion reporter #7
1078 (*cfi-1*$^{2.5kb}$*::RFP*) in WT worms and *cfi-1 (ot786)* mutants (N = 14). No significant
1079 difference was detected between WT and *cfi-1 (ot786)*, suggesting that the expression
1080 of reporter #7 (*cfi-1*$^{2.5kb}$*::RFP*) is not altered upon genetic removal of *cfi-1*. N.S.: not
1081 significant.
1082
1083
1084 **Figure 5 – figure supplement 1. Auxin-inducible depletion of LIN-39 at larval stage**
1085 **4 (L4) does not affect *cfi-1* expression in nerve cord MNs.**
1086 **A:** Representative images showing expression of LIN-39::mNG::AID after treatment with
1087 ethanol and auxin (negative control). LIN-39::mNG::AID is degraded and mNG
1088 fluorescent signal becomes undetectable in MNs, when worms are imaged after 4 days
1089 of auxin treatment. Arrowheads indicate MN nuclei in the nerve cord.
1090 **B:** Knock-down of *lin-39::mNG::AID* starting at the L4 stage (onset of auxin treatment at
1091 L4) did not affect *cfi-1*$^{2.5kb}$*::RFP* expression in adult animals 4 days later (N $\geqslant$ 13). N.S.:
1092 not significant. The number of MNs expressing *cfi-1*$^{2.5kb}$*::RFP* was quantified.
1093
1094 **Figure 5 – figure supplement 2. CFI-1 is required post-embryonically to maintain**
1095 **DA and DB neuronal identities.**
1096 **A:** CFI-1 regulates DA and DB MN identity by repressing the glutamate receptor subunit
1097 *glr-4/GluR* and possibly other genes. In *cfi-1 (-)* mutants, *glr-4/GluR* becomes
1098 ectopically activated by UNC-3 in DA and DB MNs, and these neurons adopt a mixed
1099 molecular identity.
1100 **B:** Representative images showing expression of mNG::AID::CFI-1 after treatment with
1101 ethanol and auxin. Upon two days of continuous auxin treatment (onset of treatment at
1102 L1), mNG::AID::CFI-1 is degraded and mNG expression in MNs (arrowheads) becomes
1103 undetectable
1104 **C:** Quantification of MNs expressing *glr-4::RFP* was performed on L4 worms (2 days
1105 after the onset of auxin treatment). Some mild hypomorphic effects in the expression of
1106 *glr-4::RFP* was observed in the EtOH group (negative control), potentially due to mild

1107 reduction in CFI-1 levels triggered by TIR1 even in the absence of auxin. A significant
1108 increase in the number of MNs expressing *glr-4::RFP* was evident in auxin-treated
1109 worms in comparison to control animals. WT and *cfi-1 (-)* data are also provided for
1110 comparison. N ⩾ 20. N.S.: not significant, ** $p < 0.01$.
1111
1112 **Figure 5 – figure supplement 3: Hox proteins and UNC-3 control *bnc-1* expression**
1113 **in VA and VB neurons.**
1114 **A:** Schematic summarizing the expression of *bnc-1/Bnc1* and *unc-3/Ebf* in MN subtypes
1115 of the *C. elegans* ventral nerve cord.
1116 **B:** A snapshot of UNC-3 ChIP-seq and input (negative control) signals at the *cis*-
1117 regulatory region of *bnc-1*.
1118 **C:** Quantification of expression of the endogenous reporter *bnc-1::mNG::AID* in WT,
1119 *unc-3 (n3435)*, and *lin-39 (n1760); mab-5 (e1239)* animals during L2, L4, and day 1
1120 adult stages (N ⩾ 12). *** $p < 0.001$.
1121 **D:** Representative images of the endogenous reporter *bnc-1::mNG::AID* in WT, *unc-3*
1122 *(e151)*, and *lin-39 (n1760); mab-5 (e1239)* animals during L2, L4, and day 1 adult
1123 stages. *bnc-1* is expressed in two cholinergic MN subtypes (VA and VB). Areas
1124 highlighted in dashed boxes are enlarged and presented on the right side of each
1125 picture. Arrowheads point to nuclei of VA and VB neurons that express the reporter.
1126 Above the white dashed line lies the intestine, which is autofluorescent in the green
1127 channel. Scale bar, 20 μm.
1128
1129

1130 **LEGENDS OF SUPPLEMENTARY FILES**

1131

1132 **Supplementary File 1:** Table summarizing UNC-3 ChIP-Seq signal distribution at the
1133 *cis*-regulatory regions of previously identified UNC-3 targets.

1134

1135 **Supplementary File 2:** Table summarizing the results of protein class ontology analysis
1136 over novel target genes of UNC-3. In total, 1,425 genes are classified into 25 protein
1137 classes.

1138

1139 **Supplementary File 3:** UNC-3 binds to the *cis*-regulatory region of numerous genes
1140 expressed in cholinergic MNs.

1141

1142 **Supplementary File 4:** A list of all *C. elegans* strains described in this study.

1143

1144

1145

1146

1147 **REFERENCES**

1148

1149 BAEK, M., ENRIQUEZ, J. & MANN, R. S. 2013. Dual role for Hox genes and Hox co-factors in
1150 conferring leg motoneuron survival and identity in Drosophila. *Development,* 140**,**
1151 2027-38.
1152 BLACKBURN, P. R., BARNETT, S. S., ZIMMERMANN, M. T., COUSIN, M. A., KAIWAR, C.,
1153 PINTO, E. V. F., NIU, Z., FERBER, M. J., URRUTIA, R. A., SELCEN, D., KLEE, E. W. &
1154 PICHURIN, P. N. 2017. Novel de novo variant in EBF3 is likely to impact DNA binding
1155 in a patient with a neurodevelopmental disorder and expanded phenotypes: patient
1156 report, in silico functional assessment, and review of published cases. *Cold Spring*
1157 *Harb Mol Case Stud,* 3**,** a001743.
1158 BOYLE, A. P., ARAYA, C. L., BRDLIK, C., CAYTING, P., CHENG, C., CHENG, Y., GARDNER, K.,
1159 HILLIER, L. W., JANETTE, J., JIANG, L., KASPER, D., KAWLI, T., KHERADPOUR, P.,
1160 KUNDAJE, A., LI, J. J., MA, L., NIU, W., REHM, E. J., ROZOWSKY, J., SLATTERY, M.,
1161 SPOKONY, R., TERRELL, R., VAFEADOS, D., WANG, D., WEISDEPP, P., WU, Y. C., XIE,
1162 D., YAN, K. K., FEINGOLD, E. A., GOOD, P. J., PAZIN, M. J., HUANG, H., BICKEL, P. J.,
1163 BRENNER, S. E., REINKE, V., WATERSTON, R. H., GERSTEIN, M., WHITE, K. P., KELLIS,
1164 M. & SNYDER, M. 2014. Comparative analysis of regulatory information and circuits
1165 across distant species. *Nature,* 512**,** 453-6.
1166 BRENNER, S. 1974. The genetics of Caenorhabditis elegans. *Genetics,* 77**,** 71-94.
1167 BROZOVA, E., SIMECKOVA, K., KOSTROUCH, Z., RALL, J. E. & KOSTROUCHOVA, M. 2006.
1168 NHR-40, a Caenorhabditis elegans supplementary nuclear receptor, regulates
1169 embryonic and early larval development. *Mech Dev,* 123**,** 689-701.
1170 CATELA, C. & KRATSIOS, P. 2019. Transcriptional mechanisms of motor neuron
1171 development in vertebrates and invertebrates. *Dev Biol*.
1172 CATELA, C., SHIN, M. M., LEE, D. H., LIU, J. P. & DASEN, J. S. 2016. Hox Proteins Coordinate
1173 Motor Neuron Differentiation and Connectivity Programs through Ret/Gfralpha
1174 Genes. *Cell Rep,* 14**,** 1901-15.
1175 CHAO, H. T., DAVIDS, M., BURKE, E., PAPPAS, J. G., ROSENFELD, J. A., MCCARTY, A. J., DAVIS,
1176 T., WOLFE, L., TORO, C., TIFFT, C., XIA, F., STONG, N., JOHNSON, T. K., WARR, C. G.,
1177 UNDIAGNOSED DISEASES, N., YAMAMOTO, S., ADAMS, D. R., MARKELLO, T. C., GAHL,
1178 W. A., BELLEN, H. J., WANGLER, M. F. & MALICDAN, M. C. 2017. A Syndromic
1179 Neurodevelopmental Disorder Caused by De Novo Variants in EBF3. *Am J Hum*
1180 *Genet,* 100**,** 128-137.
1181 CLARK, S. G., CHISHOLM, A. D. & HORVITZ, H. R. 1993. Control of cell fates in the central
1182 body region of C. elegans by the homeobox gene lin-39. *Cell,* 74**,** 43-55.
1183 CORBO, J. C., LAWRENCE, K. A., KARLSTETTER, M., MYERS, C. A., ABDELAZIZ, M., DIRKES,
1184 W., WEIGELT, K., SEIFERT, M., BENES, V., FRITSCHE, L. G., WEBER, B. H. &
1185 LANGMANN, T. 2010. CRX ChIP-seq reveals the cis-regulatory architecture of mouse
1186 photoreceptors. *Genome Res,* 20**,** 1512-25.
1187 COWING, D. W. & KENYON, C. 1992. Expression of the homeotic gene mab-5 during
1188 Caenorhabditis elegans embryogenesis. *Development,* 116**,** 481-90.
1189 DENERIS, E. S. & HOBERT, O. 2014. Maintenance of postmitotic neuronal cell identity. *Nat*
1190 *Neurosci,* 17**,** 899-907.
1191 DOE, C. Q. 2017. Temporal Patterning in the Drosophila CNS. *Annu Rev Cell Dev Biol,* 33**,**
1192 219-240.

1193 DUBOIS, L. & VINCENT, A. 2001. The COE--Collier/Olf1/EBF--transcription factors:
1194 structural conservation and diversity of developmental functions. *Mech Dev,* 108**,** 3-
1195 12.
1196 EASTMAN, C., HORVITZ, H. R. & JIN, Y. 1999. Coordinated transcriptional regulation of the
1197 unc-25 glutamic acid decarboxylase and the unc-47 GABA vesicular transporter by
1198 the Caenorhabditis elegans UNC-30 homeodomain protein. *J Neurosci,* 19**,** 6225-34.
1199 ELLMEIER, W., SUNSHINE, M. J., MASCHEK, R. & LITTMAN, D. R. 2002. Combined deletion of
1200 CD8 locus cis-regulatory elements affects initiation but not maintenance of CD8
1201 expression. *Immunity,* 16**,** 623-34.
1202 ESTACIO-GOMEZ, A. & DIAZ-BENJUMEA, F. J. 2014. Roles of Hox genes in the patterning of
1203 the central nervous system of Drosophila. *Fly (Austin),* 8**,** 26-32.
1204 FEDERICI, T. & BOULIS, N. M. 2006. Gene-based treatment of motor neuron diseases.
1205 *Muscle Nerve,* 33**,** 302-23.
1206 FENG, W., LI, Y., DAO, P., ABURAS, J., ISLAM, P., ELBAZ, B., KOLARZYK, A., BROWN, A. E. &
1207 KRATSIOS, P. 2020. A terminal selector prevents a Hox transcriptional switch to
1208 safeguard motor neuron identity throughout life. *Elife,* 9.
1209 FLAMES, N. & HOBERT, O. 2009. Gene regulatory logic of dopamine neuron differentiation.
1210 *Nature,* 458**,** 885-9.
1211 GARCIA-BELLIDO, A. 1975. Genetic control of wing disc development in Drosophila. *Ciba*
1212 *Found Symp,* 0**,** 161-82.
1213 GREIG, L. C., WOODWORTH, M. B., GALAZO, M. J., PADMANABHAN, H. & MACKLIS, J. D.
1214 2013. Molecular logic of neocortical projection neuron specification, development
1215 and diversity. *Nat Rev Neurosci,* 14**,** 755-69.
1216 HARMS, F. L., GIRISHA, K. M., HARDIGAN, A. A., KORTUM, F., SHUKLA, A., ALAWI, M., DALAL,
1217 A., BRADY, L., TARNOPOLSKY, M., BIRD, L. M., CEULEMANS, S., BEBIN, M., BOWLING,
1218 K. M., HIATT, S. M., LOSE, E. J., PRIMIANO, M., CHUNG, W. K., JUUSOLA, J., AKDEMIR,
1219 Z. C., BAINBRIDGE, M., CHARNG, W. L., DRUMMOND-BORG, M., ELDOMERY, M. K.,
1220 EL-HATTAB, A. W., SALEH, M. A., BEZIEAU, S., COGNE, B., ISIDOR, B., KURY, S.,
1221 LUPSKI, J. R., MYERS, R. M., COOPER, G. M. & KUTSCHE, K. 2017. Mutations in EBF3
1222 Disturb Transcriptional Profiles and Cause Intellectual Disability, Ataxia, and Facial
1223 Dysmorphism. *Am J Hum Genet,* 100**,** 117-127.
1224 HEINZ, S., BENNER, C., SPANN, N., BERTOLINO, E., LIN, Y. C., LASLO, P., CHENG, J. X., MURRE,
1225 C., SINGH, H. & GLASS, C. K. 2010. Simple combinations of lineage-determining
1226 transcription factors prime cis-regulatory elements required for macrophage and B
1227 cell identities. *Mol Cell,* 38**,** 576-89.
1228 HOBERT, O. 2002. PCR fusion-based approach to create reporter gene constructs for
1229 expression analysis in transgenic C. elegans. *Biotechniques,* 32**,** 728-30.
1230 HOBERT, O. 2008. Regulatory logic of neuronal diversity: terminal selector genes and
1231 selector motifs. *Proc Natl Acad Sci U S A,* 105**,** 20067-71.
1232 HOBERT, O. 2011. Regulation of terminal differentiation programs in the nervous system.
1233 *Annu Rev Cell Dev Biol,* 27**,** 681-96.
1234 HOBERT, O. 2016a. A map of terminal regulators of neuronal identity in Caenorhabditis
1235 elegans. *Wiley Interdiscip Rev Dev Biol,* 5**,** 474-98.
1236 HOBERT, O. 2016b. Terminal Selectors of Neuronal Identity. *Curr Top Dev Biol,* 116**,** 455-75.
1237 HOBERT, O. & KRATSIOS, P. 2019. Neuronal identity control by terminal selectors in
1238 worms, flies, and chordates. *Curr Opin Neurobiol,* 56**,** 97-105.
1239 HOUSSET, M., SAMUEL, A., ETTAICHE, M., BEMELMANS, A., BEBY, F., BILLON, N. &
1240 LAMONERIE, T. 2013. Loss of Otx2 in the adult retina disrupts retinal pigment
1241 epithelium function, causing photoreceptor degeneration. *J Neurosci,* 33**,** 9890-904.

1242 HUTLET, B., THEYS, N., COSTE, C., AHN, M. T., DOSHISHTI-AGOLLI, K., LIZEN, B. & GOFFLOT,
1243 F. 2016. Systematic expression analysis of Hox genes at adulthood reveals novel
1244 patterns in the central nervous system. *Brain Struct Funct,* 221**,** 1223-43.
1245 JAVER, A., CURRIE, M., LEE, C. W., HOKANSON, J., LI, K., MARTINEAU, C. N., YEMINI, E.,
1246 GRUNDY, L. J., LI, C., CH'NG, Q., SCHAFER, W. R., NOLLEN, E. A. A., KERR, R. &
1247 BROWN, A. E. X. 2018a. An open-source platform for analyzing and sharing worm-
1248 behavior data. *Nat Methods,* 15**,** 645-646.
1249 JAVER, A., RIPOLL-SANCHEZ, L. & BROWN, A. E. X. 2018b. Powerful and interpretable
1250 behavioural features for quantitative phenotyping of Caenorhabditis elegans. *Philos*
1251 *Trans R Soc Lond B Biol Sci,* 373.
1252 JESSELL, T. M. 2000. Neuronal specification in the spinal cord: inductive signals and
1253 transcriptional codes. *Nat Rev Genet,* 1**,** 20-9.
1254 JIN, Y., HOSKINS, R. & HORVITZ, H. R. 1994. Control of type-D GABAergic neuron
1255 differentiation by C. elegans UNC-30 homeodomain protein. *Nature,* 372**,** 780-3.
1256 JOHNSON, S. A., HARMON, K. J., SMILEY, S. G., STILL, F. M. & KAVALER, J. 2011. Discrete
1257 regulatory regions control early and late expression of D-Pax2 during external
1258 sensory organ development. *Dev Dyn,* 240**,** 1769-78.
1259 KADKHODAEI, B., ALVARSSON, A., SCHINTU, N., RAMSKOLD, D., VOLAKAKIS, N.,
1260 JOODMARDI, E., YOSHITAKE, T., KEHR, J., DECRESSAC, M., BJORKLUND, A.,
1261 SANDBERG, R., SVENNINGSSON, P. & PERLMANN, T. 2013. Transcription factor
1262 Nurr1 maintains fiber integrity and nuclear-encoded mitochondrial gene expression
1263 in dopamine neurons. *Proc Natl Acad Sci U S A,* 110**,** 2360-5.
1264 KADKHODAEI, B., ITO, T., JOODMARDI, E., MATTSSON, B., ROUILLARD, C., CARTA, M.,
1265 MURAMATSU, S., SUMI-ICHINOSE, C., NOMURA, T., METZGER, D., CHAMBON, P.,
1266 LINDQVIST, E., LARSSON, N. G., OLSON, L., BJORKLUND, A., ICHINOSE, H. &
1267 PERLMANN, T. 2009. Nurr1 is required for maintenance of maturing and adult
1268 midbrain dopamine neurons. *J Neurosci,* 29**,** 15923-32.
1269 KARLSSON, D., BAUMGARDT, M. & THOR, S. 2010. Segment-specific neuronal subtype
1270 specification by the integration of anteroposterior and temporal cues. *PLoS Biol,* 8**,**
1271 e1000368.
1272 KERK, S. Y., KRATSIOS, P., HART, M., MOURAO, R. & HOBERT, O. 2017. Diversification of C.
1273 elegans Motor Neuron Identity via Selective Effector Gene Repression. *Neuron,* 93**,**
1274 80-98.
1275 KIM, K., COLOSIMO, M. E., YEUNG, H. & SENGUPTA, P. 2005. The UNC-3 Olf/EBF protein
1276 represses alternate neuronal programs to specify chemosensory neuron identity.
1277 *Dev Biol,* 286**,** 136-48.
1278 KONSTANTINIDES, N., KAPURALIN, K., FADIL, C., BARBOZA, L., SATIJA, R. & DESPLAN, C.
1279 2018. Phenotypic Convergence: Distinct Transcription Factors Regulate Common
1280 Terminal Features. *Cell,* 174**,** 622-635 e13.
1281 KRATSIOS, P., KERK, S. Y., CATELA, C., LIANG, J., VIDAL, B., BAYER, E. A., FENG, W., DE LA
1282 CRUZ, E. D., CROCI, L., CONSALEZ, G. G., MIZUMOTO, K. & HOBERT, O. 2017. An
1283 intersectional gene regulatory strategy defines subclass diversity of C. elegans
1284 motor neurons. *Elife,* 6.
1285 KRATSIOS, P., PINAN-LUCARRE, B., KERK, S. Y., WEINREB, A., BESSEREAU, J. L. & HOBERT,
1286 O. 2015. Transcriptional coordination of synaptogenesis and neurotransmitter
1287 signaling. *Curr Biol,* 25**,** 1282-95.
1288 KRATSIOS, P., STOLFI, A., LEVINE, M. & HOBERT, O. 2012. Coordinated regulation of
1289 cholinergic motor neuron traits through a conserved terminal selector gene. *Nat*
1290 *Neurosci,* 15**,** 205-14.

1291 LANGMEAD, B. & SALZBERG, S. L. 2012. Fast gapped-read alignment with Bowtie 2. *Nat*
1292 *Methods,* 9**,** 357-9.
1293 LEYVA-DIAZ, E. & HOBERT, O. 2019. Transcription factor autoregulation is required for
1294 acquisition and maintenance of neuronal identity. *Development,* 146.
1295 LIU, J. & FIRE, A. 2000. Overlapping roles of two Hox genes and the exd ortholog ceh-20 in
1296 diversification of the C. elegans postembryonic mesoderm. *Development,* 127**,** 5179-
1297 90.
1298 LODATO, S. & ARLOTTA, P. 2015. Generating neuronal diversity in the mammalian cerebral
1299 cortex. *Annu Rev Cell Dev Biol,* 31**,** 699-720.
1300 LOPES, R., VERHEY VAN WIJK, N., NEVES, G. & PACHNIS, V. 2012. Transcription factor LIM
1301 homeobox 7 (Lhx7) maintains subtype identity of cholinergic interneurons in the
1302 mammalian striatum. *Proc Natl Acad Sci U S A,* 109**,** 3119-24.
1303 MALOOF, J. N. & KENYON, C. 1998. The Hox gene lin-39 is required during C. elegans vulval
1304 induction to select the outcome of Ras signaling. *Development,* 125**,** 181-90.
1305 MANZANARES, M., BEL-VIALAR, S., ARIZA-MCNAUGHTON, L., FERRETTI, E., MARSHALL, H.,
1306 MACONOCHIE, M. M., BLASI, F. & KRUMLAUF, R. 2001. Independent regulation of
1307 initiation and maintenance phases of Hoxa3 expression in the vertebrate hindbrain
1308 involve auto- and cross-regulatory mechanisms. *Development,* 128**,** 3595-607.
1309 MAYER, C., HAFEMEISTER, C., BANDLER, R. C., MACHOLD, R., BATISTA BRITO, R., JAGLIN,
1310 X., ALLAWAY, K., BUTLER, A., FISHELL, G. & SATIJA, R. 2018. Developmental
1311 diversification of cortical inhibitory interneurons. *Nature,* 555**,** 457-462.
1312 MI, D., LI, Z., LIM, L., LI, M., MOISSIDIS, M., YANG, Y., GAO, T., HU, T. X., PRATT, T., PRICE, D. J.,
1313 SESTAN, N. & MARIN, O. 2018. Early emergence of cortical interneuron diversity in
1314 the mouse embryo. *Science,* 360**,** 81-85.
1315 MI, H., MURUGANUJAN, A., CASAGRANDE, J. T. & THOMAS, P. D. 2013. Large-scale gene
1316 function analysis with the PANTHER classification system. *Nat Protoc,* 8**,** 1551-66.
1317 MIGUEL-ALIAGA, I. & THOR, S. 2004. Segment-specific prevention of pioneer neuron
1318 apoptosis by cell-autonomous, postmitotic Hox gene activity. *Development,* 131**,**
1319 6093-105.
1320 MORIS-SANZ, M., ESTACIO-GOMEZ, A., SANCHEZ-HERRERO, E. & DIAZ-BENJUMEA, F. J.
1321 2015. The study of the Bithorax-complex genes in patterning CCAP neurons reveals
1322 a temporal control of neuronal differentiation by Abd-B. *Biol Open,* 4**,** 1132-42.
1323 OKATY, B. W., FRERET, M. E., ROOD, B. D., BRUST, R. D., HENNESSY, M. L., DEBAIROS, D.,
1324 KIM, J. C., COOK, M. N. & DYMECKI, S. M. 2015. Multi-Scale Molecular Deconstruction
1325 of the Serotonin Neuron System. *Neuron,* 88**,** 774-91.
1326 PEREIRA, L., KRATSIOS, P., SERRANO-SAIZ, E., SHEFTEL, H., MAYO, A. E., HALL, D. H.,
1327 WHITE, J. G., LEBOEUF, B., GARCIA, L. R., ALON, U. & HOBERT, O. 2015. A cellular and
1328 regulatory map of the cholinergic nervous system of C. elegans. *Elife,* 4.
1329 PERRY, M., KONSTANTINIDES, N., PINTO-TEIXEIRA, F. & DESPLAN, C. 2017. Generation and
1330 Evolution of Neural Cell Types and Circuits: Insights from the Drosophila Visual
1331 System. *Annu Rev Genet,* 51**,** 501-527.
1332 PFEFFER, P. L., PAYER, B., REIM, G., DI MAGLIANO, M. P. & BUSSLINGER, M. 2002. The
1333 activation and maintenance of Pax2 expression at the mid-hindbrain boundary is
1334 controlled by separate enhancers. *Development,* 129**,** 307-18.
1335 PHILIPPIDOU, P. & DASEN, J. S. 2013. Hox genes: choreographers in neural development,
1336 architects of circuit organization. *Neuron,* 80**,** 12-34.
1337 PIKKARAINEN, S., TOKOLA, H., KERKELA, R. & RUSKOAHO, H. 2004. GATA transcription
1338 factors in the developing and adult heart. *Cardiovasc Res,* 63**,** 196-207.

1339 POCOCK, R., MIONE, M., HUSSAIN, S., MAXWELL, S., PONTECORVI, M., ASLAM, S., GERRELLI,
1340 D., SOWDEN, J. C. & WOOLLARD, A. 2008. Neuronal function of Tbx20 conserved
1341 from nematodes to vertebrates. *Dev Biol,* 317**,** 671-85.
1342 PRASAD, B. C., YE, B., ZACKHARY, R., SCHRADER, K., SEYDOUX, G. & REED, R. R. 1998. unc-3,
1343 a gene required for axonal guidance in Caenorhabditis elegans, encodes a member of
1344 the O/E family of transcription factors. *Development,* 125**,** 1561-8.
1345 RAMIREZ, F., RYAN, D. P., GRUNING, B., BHARDWAJ, V., KILPERT, F., RICHTER, A. S., HEYNE,
1346 S., DUNDAR, F. & MANKE, T. 2016. deepTools2: a next generation web server for
1347 deep-sequencing data analysis. *Nucleic Acids Res,* 44**,** W160-5.
1348 RHEE, H. S., CLOSSER, M., GUO, Y., BASHKIROVA, E. V., TAN, G. C., GIFFORD, D. K. &
1349 WICHTERLE, H. 2016. Expression of Terminal Effector Genes in Mammalian
1350 Neurons Is Maintained by a Dynamic Relay of Transient Enhancers. *Neuron,* 92**,**
1351 1252-1265.
1352 SABARIS, G., LAIKER, I., PREGER-BEN NOON, E. & FRANKEL, N. 2019. Actors with Multiple
1353 Roles: Pleiotropic Enhancers and the Paradigm of Enhancer Modularity. *Trends*
1354 *Genet,* 35**,** 423-433.
1355 SCHINDELIN, J., ARGANDA-CARRERAS, I., FRISE, E., KAYNIG, V., LONGAIR, M., PIETZSCH, T.,
1356 PREIBISCH, S., RUEDEN, C., SAALFELD, S., SCHMID, B., TINEVEZ, J. Y., WHITE, D. J.,
1357 HARTENSTEIN, V., ELICEIRI, K., TOMANCAK, P. & CARDONA, A. 2012. Fiji: an open-
1358 source platform for biological-image analysis. *Nat Methods,* 9**,** 676-82.
1359 SCOTT, M. M., KRUEGER, K. C. & DENERIS, E. S. 2005. A differentially autoregulated Pet-1
1360 enhancer region is a critical target of the transcriptional cascade that governs
1361 serotonin neuron development. *J Neurosci,* 25**,** 2628-36.
1362 SETH R TAYLOR, G. S., MOLLY REILLY, LORI GLENWINKEL, ABIGAIL POFF, REBECCA
1363 MCWHIRTER, CHUAN XU, ALEXIS WEINREB, MANASA BASAVARAJU, STEVEN J
1364 COOK, ALEC BARRETT, ALEXANDER ABRAMS, BERTA VIDAL, CYRIL CROS, IBNUL
1365 RAFI, NENAD SESTAN, MARC HAMMARLUND, OLIVER HOBERT, DAVID M. MILLER
1366 III 2019. Expression profiling of the mature C. elegans nervous system by single-cell
1367 RNA-Sequencing. *bioRxiv*.
1368 SHAHAM, S. & BARGMANN, C. I. 2002. Control of neuronal subtype identity by the C.
1369 elegans ARID protein CFI-1. *Genes Dev,* 16**,** 972-83.
1370 SHEN, L., SHAO, N., LIU, X. & NESTLER, E. 2014. ngs.plot: Quick mining and visualization of
1371 next-generation sequencing data by integrating genomic databases. *BMC Genomics,*
1372 15**,** 284.
1373 SLEVEN, H., WELSH, S. J., YU, J., CHURCHILL, M. E., WRIGHT, C. F., HENDERSON, A.,
1374 HORVATH, R., RANKIN, J., VOGT, J., MAGEE, A., MCCONNELL, V., GREEN, A., KING, M.
1375 D., COX, H., ARMSTRONG, L., LEHMAN, A., NELSON, T. N., DECIPHERING
1376 DEVELOPMENTAL DISORDERS, S., STUDY, C., WILLIAMS, J., CLOUSTON, P.,
1377 HAGMAN, J. & NEMETH, A. H. 2017. De Novo Mutations in EBF3 Cause a
1378 Neurodevelopmental Syndrome. *Am J Hum Genet,* 100**,** 138-150.
1379 SOLER, C., HAN, J. & TAYLOR, M. V. 2012. The conserved transcription factor Mef2 has
1380 multiple roles in adult Drosophila musculature formation. *Development,* 139**,** 1270-
1381 5.
1382 TAKAHASHI, Y., HAMADA, J., MURAKAWA, K., TAKADA, M., TADA, M., NOGAMI, I., HAYASHI,
1383 N., NAKAMORI, S., MONDEN, M., MIYAMOTO, M., KATOH, H. & MORIUCHI, T. 2004.
1384 Expression profiles of 39 HOX genes in normal human adult organs and anaplastic
1385 thyroid cancer cell lines by quantitative real-time RT-PCR system. *Exp Cell Res,* 293**,**
1386 144-53.

1387 TREIBER, N., TREIBER, T., ZOCHER, G. & GROSSCHEDL, R. 2010a. Structure of an Ebf1:DNA
1388 complex reveals unusual DNA recognition and structural homology with Rel
1389 proteins. *Genes Dev,* 24**,** 2270-5.
1390 TREIBER, T., MANDEL, E. M., POTT, S., GYORY, I., FIRNER, S., LIU, E. T. & GROSSCHEDL, R.
1391 2010b. Early B cell factor 1 regulates B cell gene networks by activation, repression,
1392 and transcription- independent poising of chromatin. *Immunity,* 32**,** 714-25.
1393 WANG, M. M. & REED, R. R. 1993. Molecular cloning of the olfactory neuronal transcription
1394 factor Olf-1 by genetic selection in yeast. *Nature,* 364**,** 121-6.
1395 WANG, M. M., TSAI, R. Y., SCHRADER, K. A. & REED, R. R. 1993. Genes encoding components
1396 of the olfactory signal transduction cascade contain a DNA binding site that may
1397 direct neuronal expression. *Mol Cell Biol,* 13**,** 5805-13.
1398 WANG, S. S., TSAI, R. Y. & REED, R. R. 1997. The characterization of the Olf-1/EBF-like HLH
1399 transcription factor family: implications in olfactory gene regulation and neuronal
1400 development. *J Neurosci,* 17**,** 4149-58.
1401 WIESENFAHRT, T., BERG, J. Y., OSBORNE NISHIMURA, E., ROBINSON, A. G., GOSZCZYNSKI,
1402 B., LIEB, J. D. & MCGHEE, J. D. 2016. The function and regulation of the GATA factor
1403 ELT-2 in the C. elegans endoderm. *Development,* 143**,** 483-91.
1404 WYLER, S. C., SPENCER, W. C., GREEN, N. H., ROOD, B. D., CRAWFORD, L., CRAIGE, C.,
1405 GRESCH, P., MCMAHON, D. G., BECK, S. G. & DENERIS, E. 2016. Pet-1 Switches
1406 Transcriptional Targets Postnatally to Regulate Maturation of Serotonin Neuron
1407 Excitability. *J Neurosci,* 36**,** 1758-74.
1408 XUE, D., FINNEY, M., RUVKUN, G. & CHALFIE, M. 1992. Regulation of the mec-3 gene by the
1409 C.elegans homeoproteins UNC-86 and MEC-3. *EMBO J,* 11**,** 4969-79.
1410 YEMINI, E., JUCIKAS, T., GRUNDY, L. J., BROWN, A. E. & SCHAFER, W. R. 2013. A database of
1411 Caenorhabditis elegans behavioral phenotypes. *Nat Methods,* 10**,** 877-9.
1412 YU, B., WANG, X., WEI, S., FU, T., DZAKAH, E. E., WAQAS, A., WALTHALL, W. W. & SHAN, G.
1413 2017. Convergent Transcriptional Programs Regulate cAMP Levels in C. elegans
1414 GABAergic Motor Neurons. *Dev Cell,* 43**,** 212-226 e7.
1415 YU, G., WANG, L. G. & HE, Q. Y. 2015. ChIPseeker: an R/Bioconductor package for ChIP peak
1416 annotation, comparison and visualization. *Bioinformatics,* 31**,** 2382-3.
1417 ZHANG, L., WARD, J. D., CHENG, Z. & DERNBURG, A. F. 2015. The auxin-inducible
1418 degradation (AID) system enables versatile conditional protein depletion in C.
1419 elegans. *Development,* 142**,** 4374-84.
1420 ZHENG, C., JIN, F. Q. & CHALFIE, M. 2015. Hox Proteins Act as Transcriptional Guarantors to
1421 Ensure Terminal Differentiation. *Cell Rep,* 13**,** 1343-1352.
1422 ZHOU, Q., LIU, M., XIA, X., GONG, T., FENG, J., LIU, W., LIU, Y., ZHEN, B., WANG, Y., DING, C. &
1423 QIN, J. 2017. A mouse tissue transcription factor atlas. *Nat Commun,* 8**,** 15089.
1424

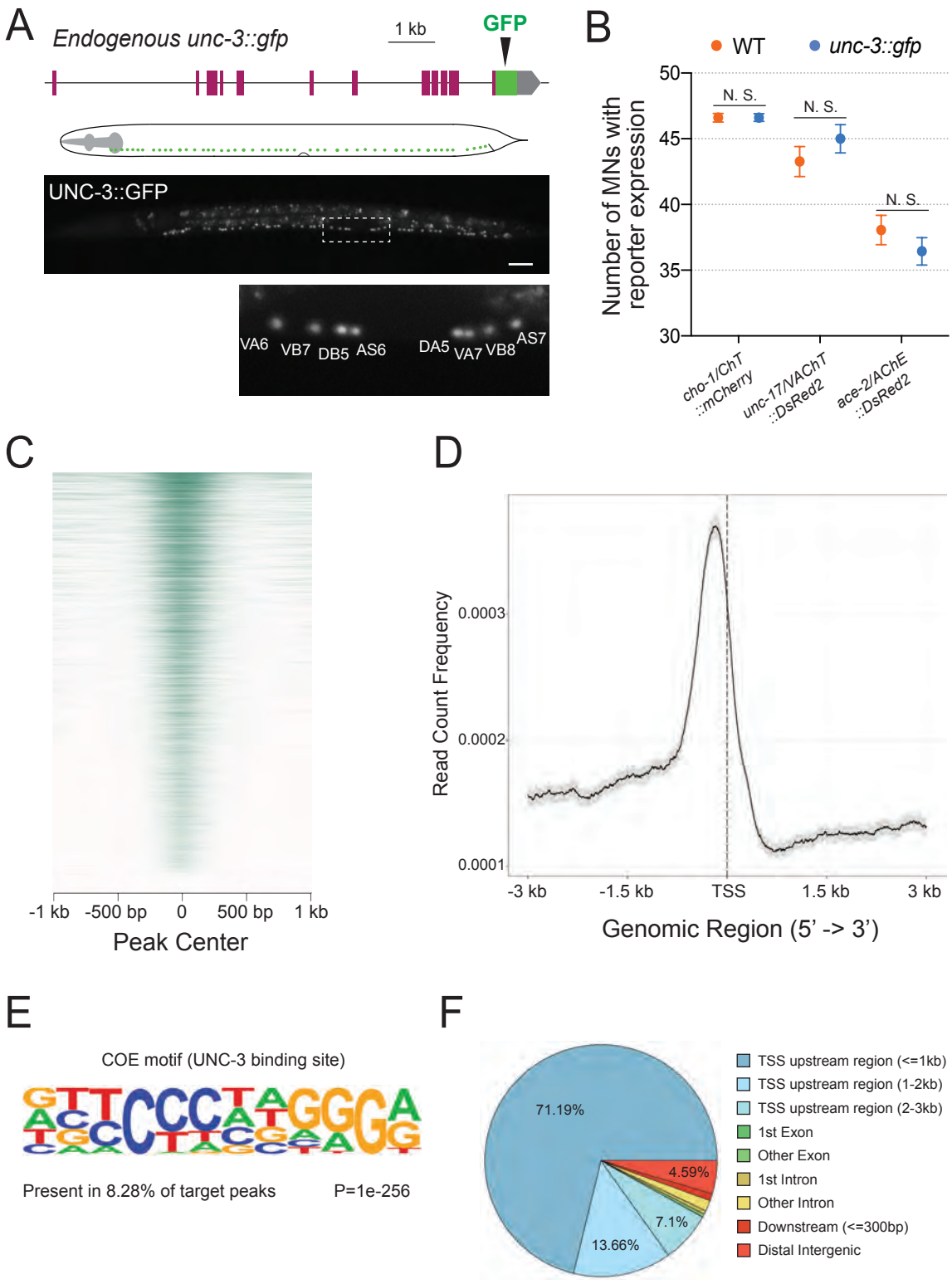
A
Endogenous unc-3::gfp
1 kb
GFP
UNC-3::GFP
VA6
VB7
DB5
AS6
DA5
VA7
VB8
AS7
B
WT
unc-3::gfp
Number of MNs with reporter expression
50
45
40
35
30
N. S.
N. S.
N. S.
cho-1/ChT ::mCherry
unc-17/VAChT ::DsRed2
ace-2/AChE ::DsRed2
C
-1 kb
-500 bp
0
500 bp
1 kb
Peak Center
D
Read Count Frequency
0.0003
0.0002
0.0001
-3 kb
-1.5 kb
TSS
1.5 kb
3 kb
Genomic Region (5' -> 3')
E
COE motif (UNC-3 binding site)
Present in 8.28% of target peaks
P=1e-256
F
71.19%
4.59%
7.1%
13.66%
TSS upstream region (<=1kb)
TSS upstream region (1-2kb)
TSS upstream region (2-3kb)
1st Exon
Other Exon
1st Intron
Other Intron
Downstream (<=300bp)
Distal Intergenic

Figure 1 - figure supplement 1

A

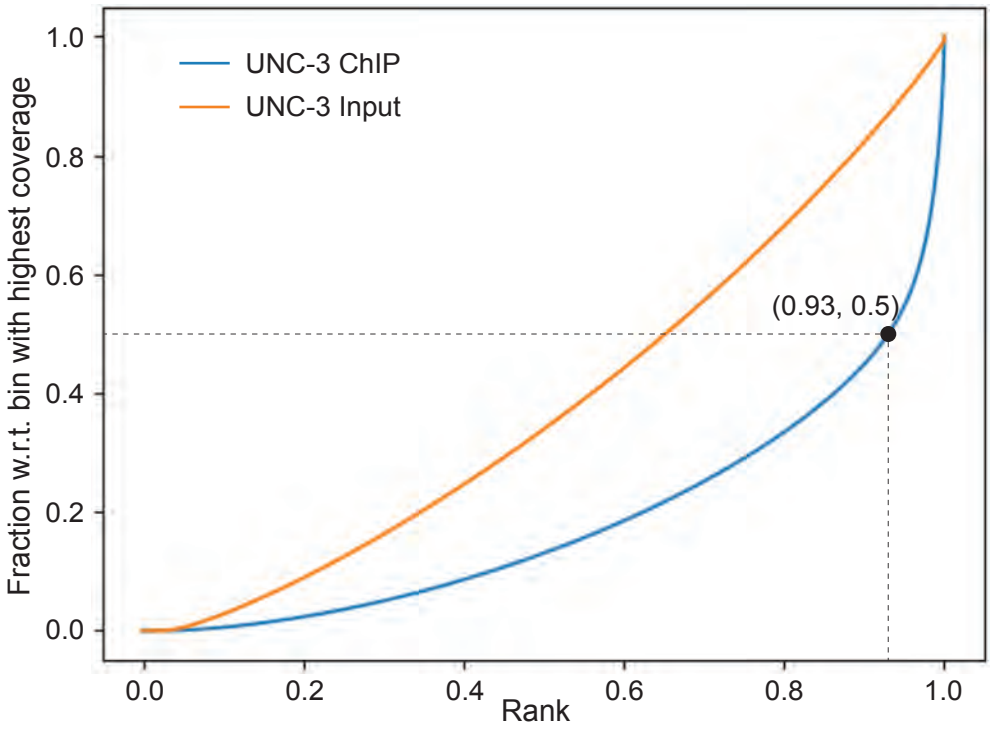

B

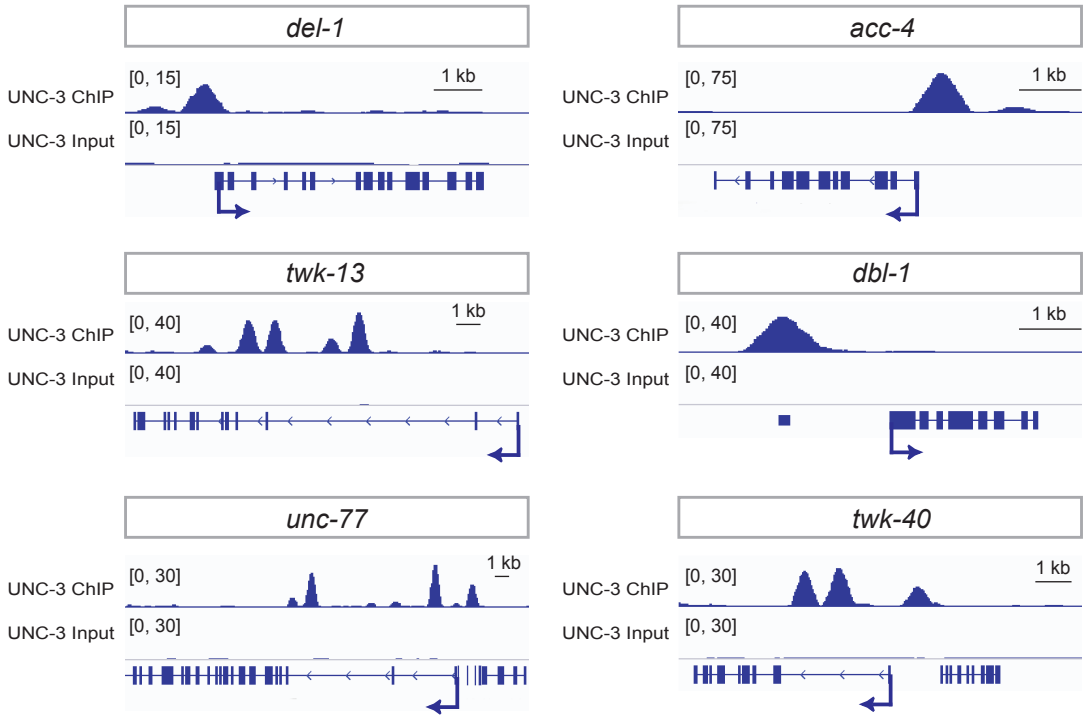

A

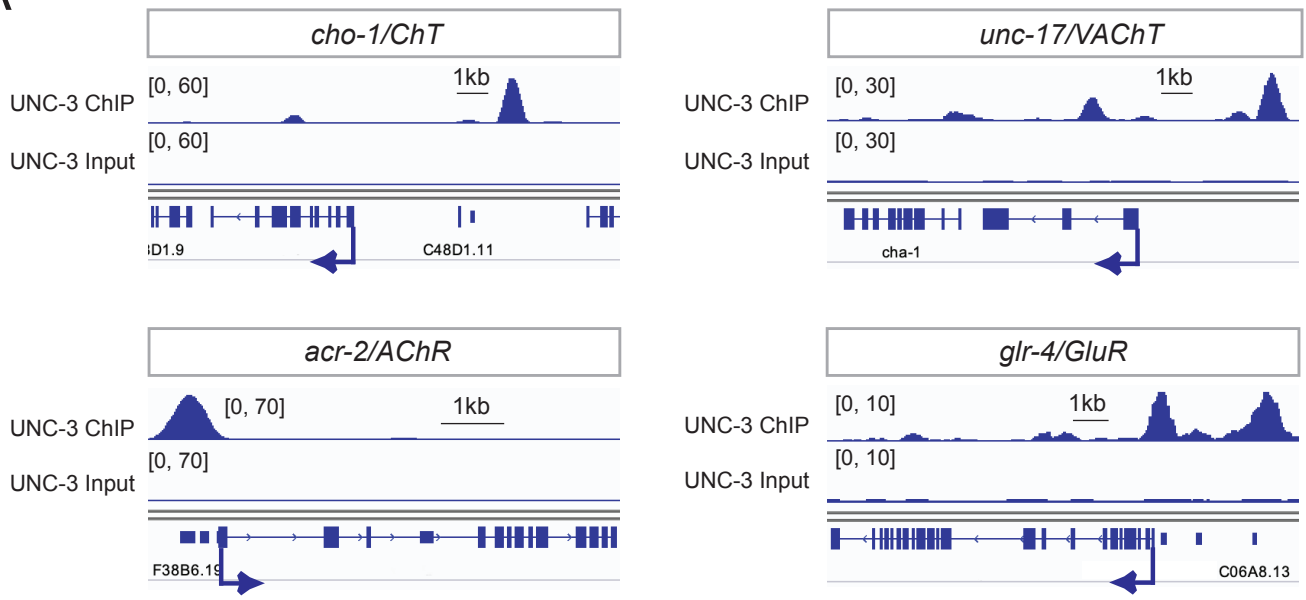
cho-1/ChT
UNC-3 ChIP
UNC-3 Input
[0, 60]
[0, 60]
1kb
C48D1.11
unc-17/VAChT
UNC-3 ChIP
UNC-3 Input
[0, 30]
[0, 30]
1kb
cha-1
acr-2/AChR
UNC-3 ChIP
UNC-3 Input
[0, 70]
[0, 70]
1kb
glr-4/GluR
UNC-3 ChIP
UNC-3 Input
[0, 10]
[0, 10]
1kb
C06A8.13

B

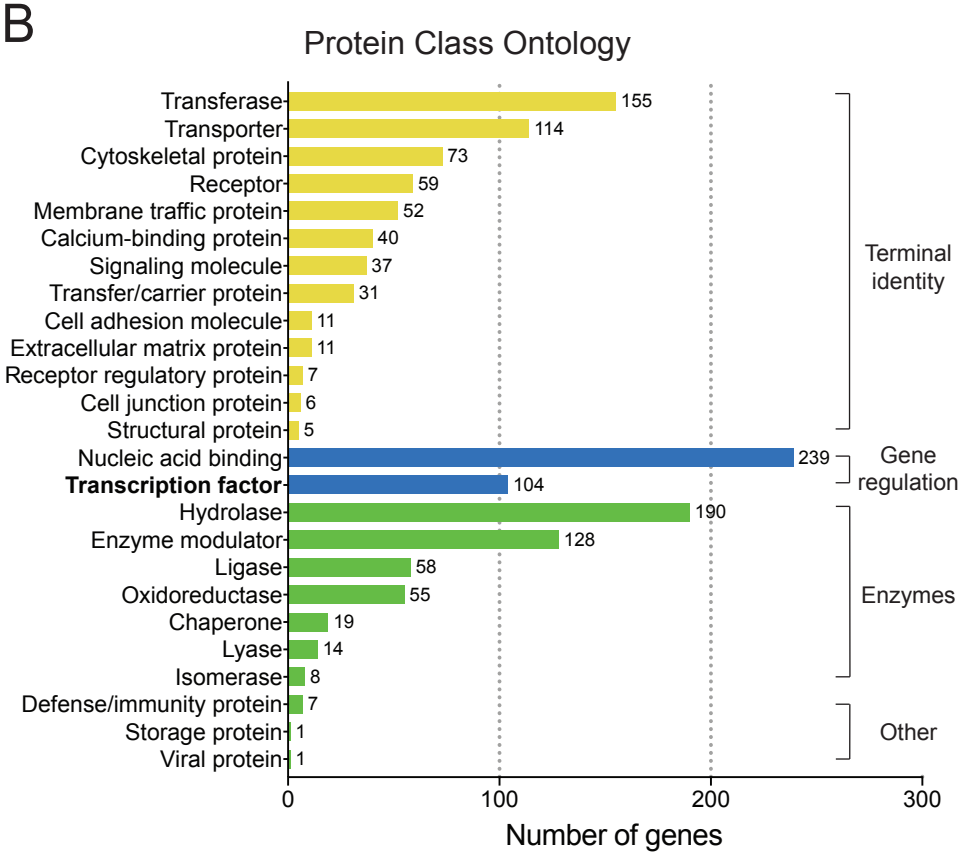
Protein Class Ontology
Transferase 155
Transporter 114
Cytoskeletal protein 73
Receptor 59
Membrane traffic protein 52
Calcium-binding protein 40
Signaling molecule 37
Transfer/carrier protein 31
Cell adhesion molecule 11
Extracellular matrix protein 11
Receptor regulatory protein 7
Cell junction protein 6
Structural protein 5
Nucleic acid binding 239
Transcription factor 104
Hydrolase 190
Enzyme modulator 128
Ligase 58
Oxidoreductase 55
Chaperone 19
Lyase 14
Isomerase 8
Defense/immunity protein 7
Storage protein 1
Viral protein 1
Terminal identity
Gene regulation
Enzymes
Other
0
100
200
300
Number of genes

C

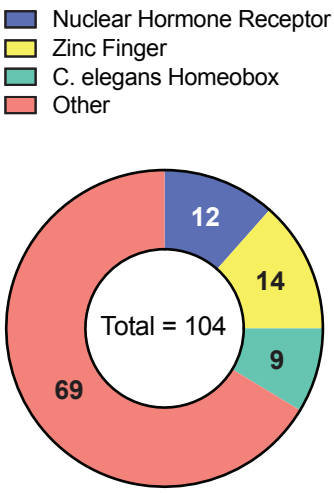
Nuclear Hormone Receptor
Zinc Finger
C. elegans Homeobox
Other
12
14
9
69
Total = 104

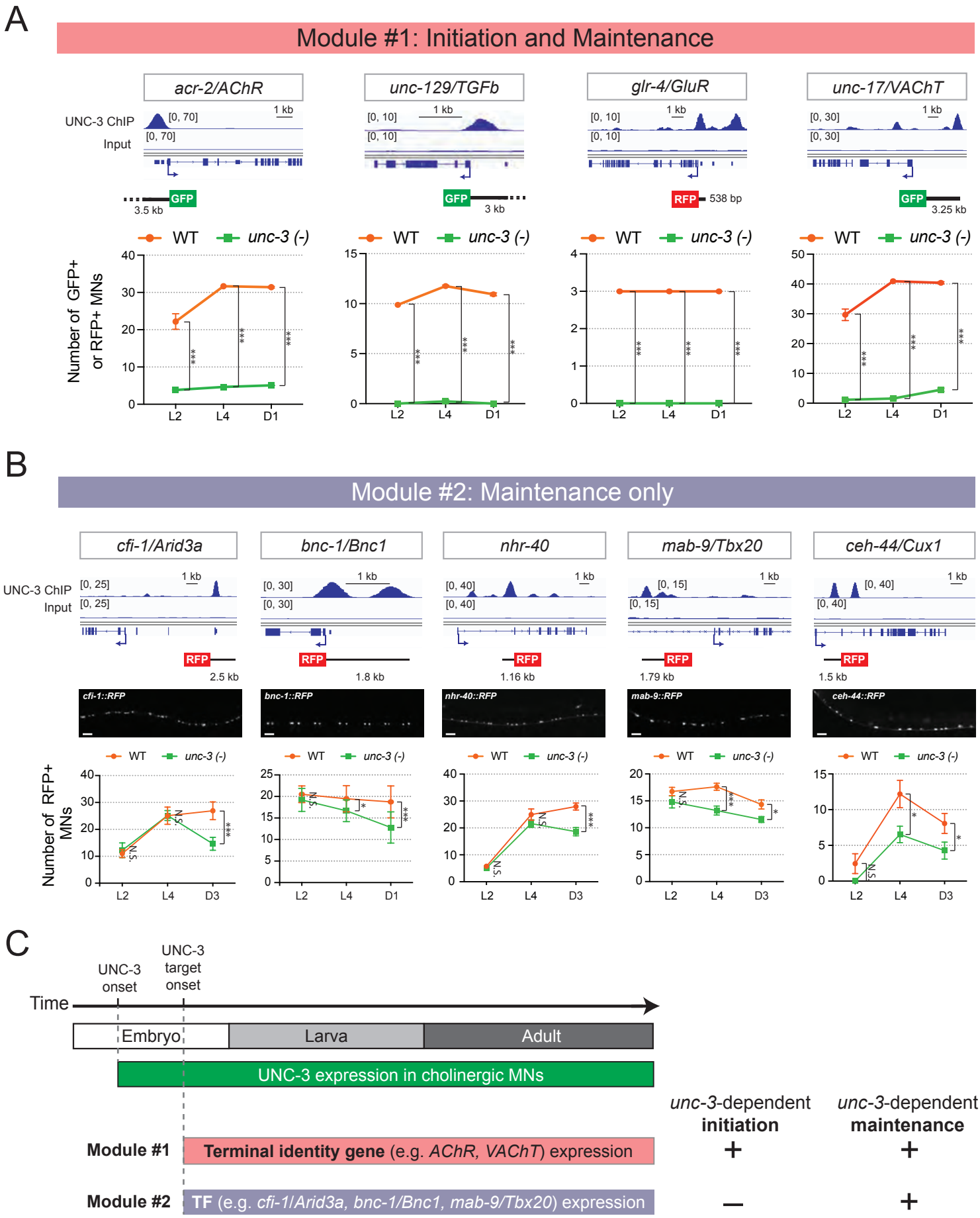
A
Module #1: Initiation and Maintenance
acr-2/AChR
unc-129/TGFb
glr-4/GluR
unc-17/VAChT
UNC-3 ChIP
Input
1 kb
GFP
RFP
538 bp
3.5 kb
3 kb
3.25 kb
WT
unc-3 (-)
Number of GFP+ or RFP+ MNs
L2
L4
D1
B
Module #2: Maintenance only
cfi-1/Arid3a
bnc-1/Bnc1
nhr-40
mab-9/Tbx20
ceh-44/Cux1
2.5 kb
1.8 kb
1.16 kb
1.79 kb
1.5 kb
cfi-1::RFP
bnc-1::RFP
nhr-40::RFP
mab-9::RFP
ceh-44::RFP
Number of RFP+ MNs
L2
L4
D3
C
UNC-3 onset
UNC-3 target onset
Time
Embryo
Larva
Adult
UNC-3 expression in cholinergic MNs
unc-3-dependent initiation
unc-3-dependent maintenance
Module #1
Terminal identity gene (e.g. AChR, VAChT) expression
Module #2
TF (e.g. cfi-1/Arid3a, bnc-1/Bnc1, mab-9/Tbx20) expression

Figure 3 - figure supplement 1

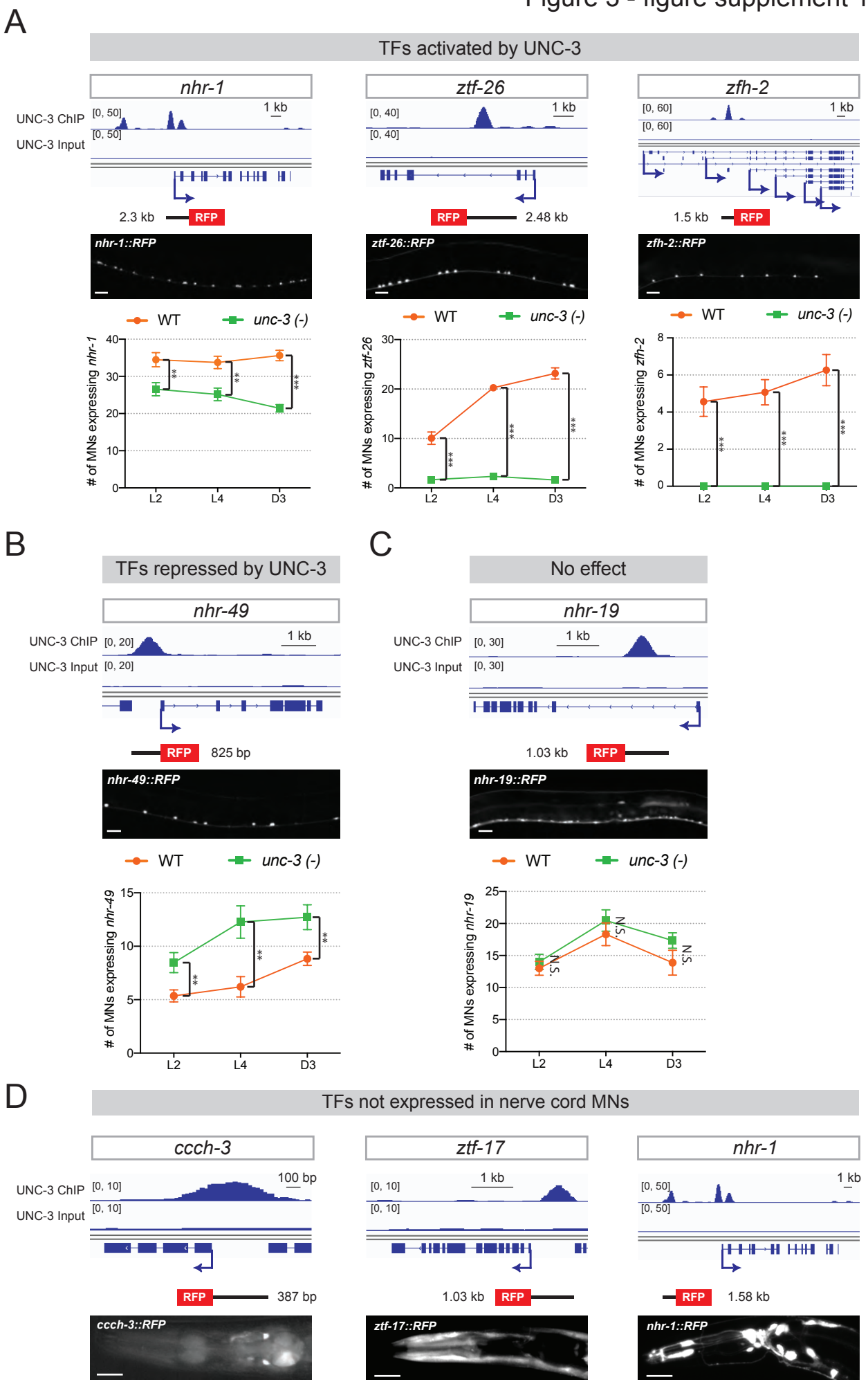

Figure 4

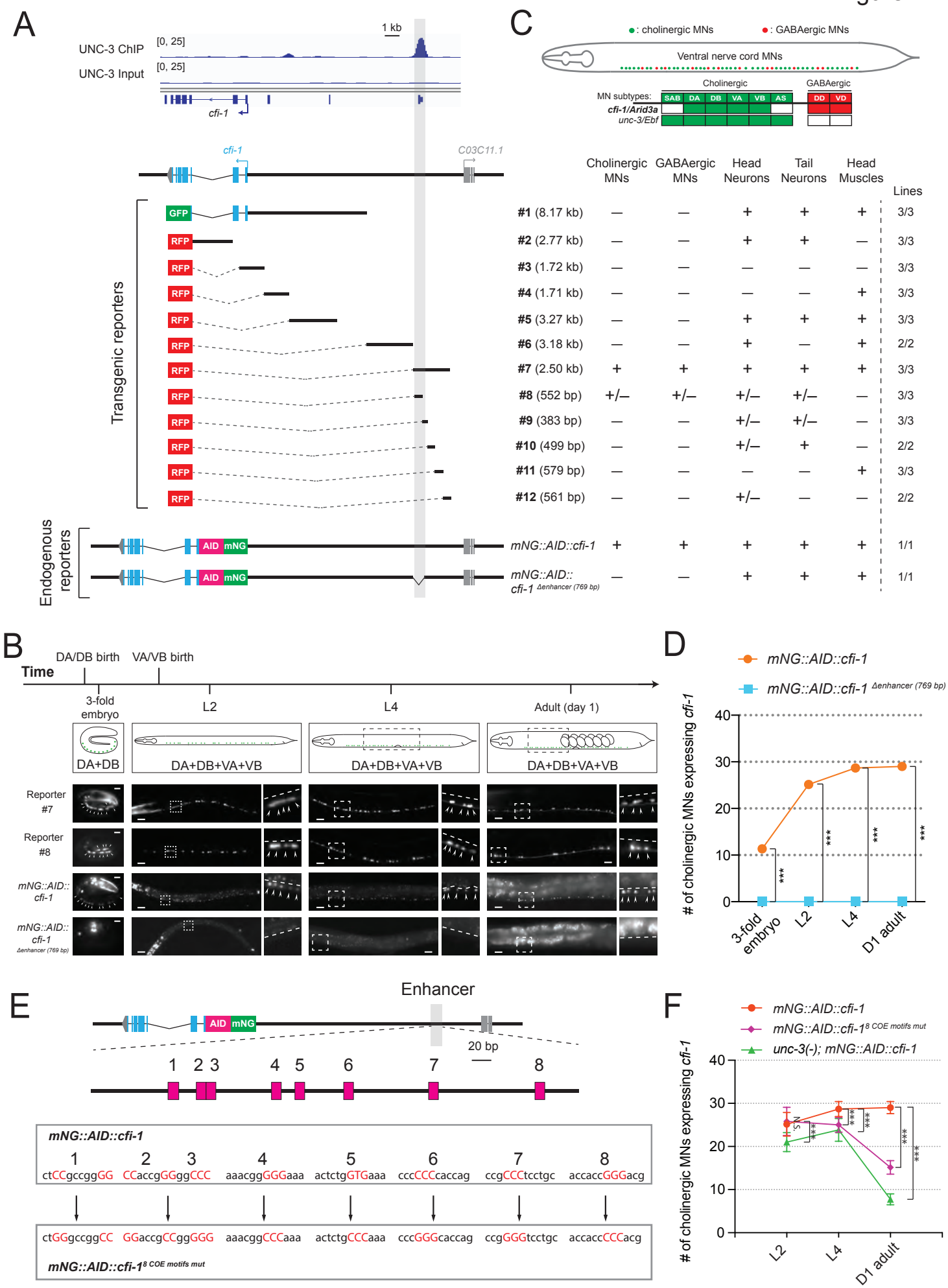

A
1 kb
UNC-3 ChIP
[0, 25]
UNC-3 Input
[0, 25]
cfi-1
cfi-1
C03C11.1
Transgenic reporters
GFP
RFP
Endogenous reporters
AID mNG
C
: cholinergic MNs
: GABAergic MNs
Ventral nerve cord MNs
Cholinergic
GABAergic
MN subtypes:
SAB DA DB VA VB AS
DD VD
cfi-1/Arid3a
unc-3/Ebf
Cholinergic MNs
GABAergic MNs
Head Neurons
Tail Neurons
Head Muscles
Lines
#1 (8.17 kb) — — + + + 3/3
#2 (2.77 kb) — — + + — 3/3
#3 (1.72 kb) — — — — — 3/3
#4 (1.71 kb) — — — — + 3/3
#5 (3.27 kb) — — + + + 3/3
#6 (3.18 kb) — — + — + 2/2
#7 (2.50 kb) + + + + + 3/3
#8 (552 bp) +/– +/– +/– +/– — 3/3
#9 (383 bp) — — +/– +/– — 3/3
#10 (499 bp) — — +/– + — 2/2
#11 (579 bp) — — — — + 3/3
#12 (561 bp) — — +/– — — 2/2
mNG::AID::cfi-1 + + + + + 1/1
mNG::AID::cfi-1 Δenhancer (769 bp) — — + + + 1/1
B
Time
DA/DB birth
VA/VB birth
3-fold embryo
L2
L4
Adult (day 1)
DA+DB
DA+DB+VA+VB
DA+DB+VA+VB
DA+DB+VA+VB
Reporter #7
Reporter #8
mNG::AID::cfi-1
mNG::AID::cfi-1 Δenhancer (769 bp)
D
mNG::AID::cfi-1
mNG::AID::cfi-1 Δenhancer (769 bp)
# of cholinergic MNs expressing cfi-1
40
30
20
10
0
***
3-fold embryo
L2
L4
D1 adult
E
Enhancer
AID mNG
20 bp
1 2 3 4 5 6 7 8
mNG::AID::cfi-1
1 2 3 4 5 6 7 8
ctCCgccggGG CCaccgGGggCCC aaacggGGGaaa actctgGTGaaa cccCCCcaccag ccgCCCtcctgc accaccGGGacg
ctGGgccggCC GGaccgCCggGGG aaacggCCCaaa actctgCCCaaa cccGGGcaccag ccgGGGtcctgc accaccCCCacg
mNG::AID::cfi-1 8 COE motifs mut
F
mNG::AID::cfi-1
mNG::AID::cfi-1 8 COE motifs mut
unc-3(-); mNG::AID::cfi-1
# of cholinergic MNs expressing cfi-1
40
30
20
10
0
N.S.
***
L2
L4
D1 adult

Figure 4 - figure supplement 1

A

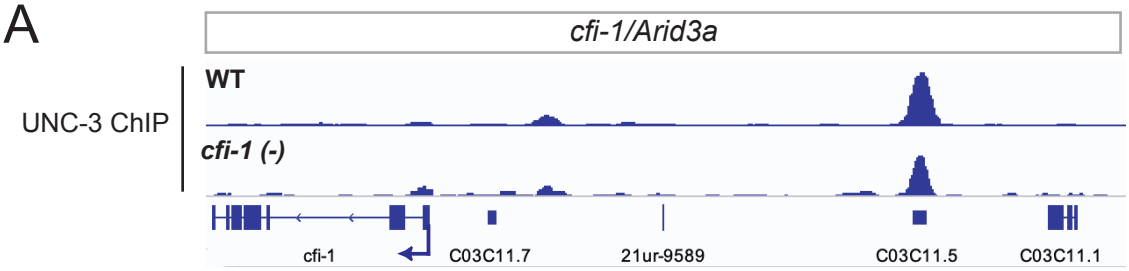

B

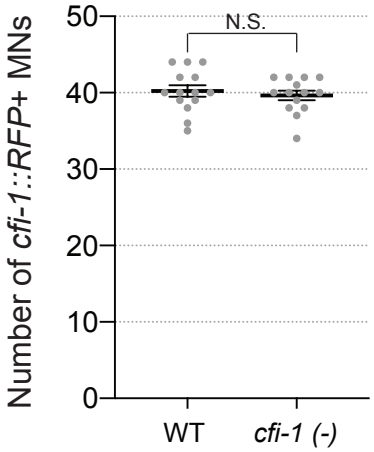

Figure 5

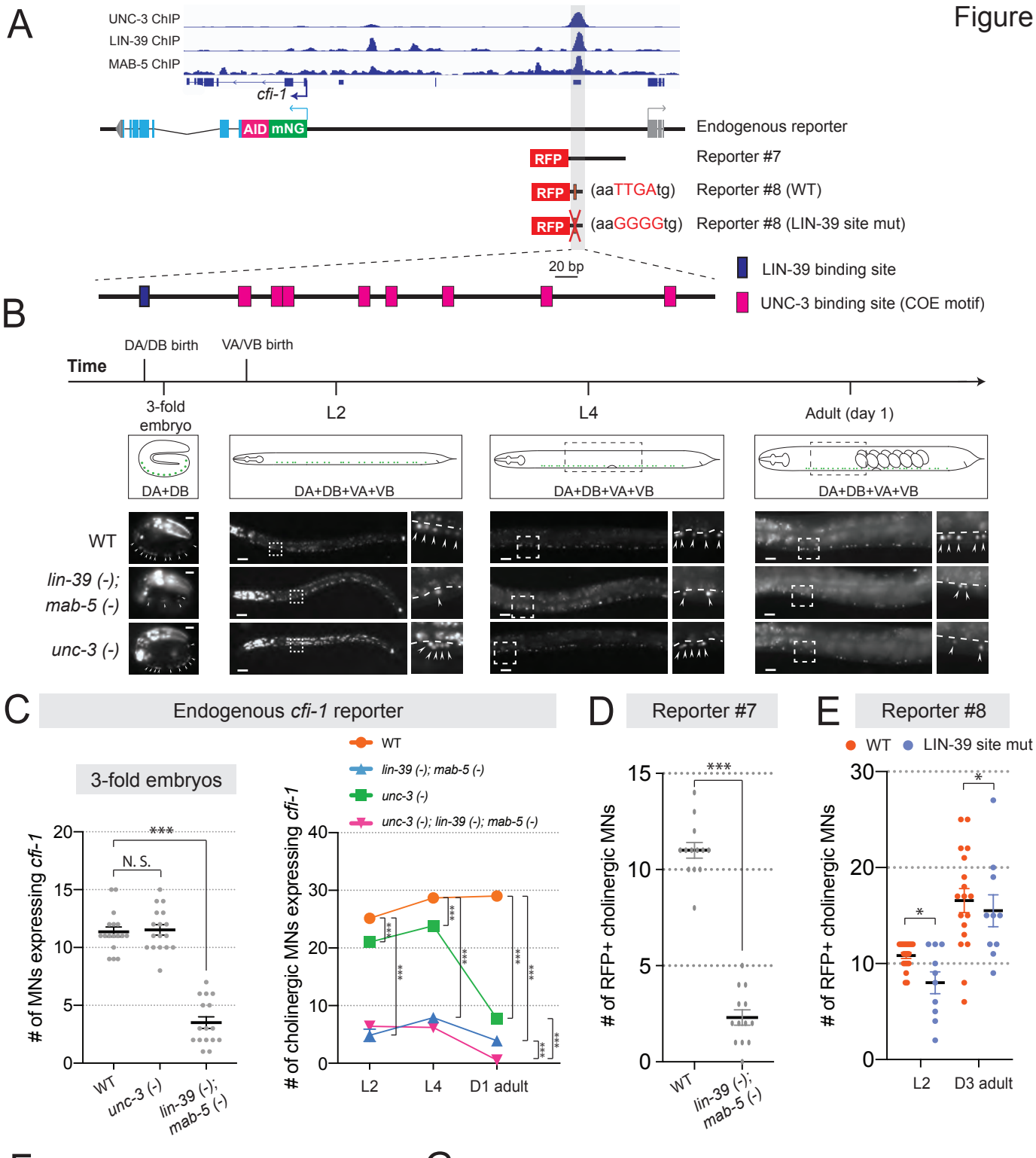
A
UNC-3 ChIP
LIN-39 ChIP
MAB-5 ChIP
cfi-1
AID
mNG
Endogenous reporter
RFP
Reporter #7
(aaTTGAtg)
Reporter #8 (WT)
(aaGGGGtg)
Reporter #8 (LIN-39 site mut)
20 bp
LIN-39 binding site
UNC-3 binding site (COE motif)
B
Time
DA/DB birth
VA/VB birth
3-fold embryo
L2
L4
Adult (day 1)
DA+DB
DA+DB+VA+VB
WT
lin-39 (-); mab-5 (-)
unc-3 (-)
C
Endogenous cfi-1 reporter
3-fold embryos
# of MNs expressing cfi-1
N. S.
***
WT
unc-3 (-)
lin-39 (-); mab-5 (-)
# of cholinergic MNs expressing cfi-1
lin-39 (-); mab-5 (-)
unc-3 (-); lin-39 (-); mab-5 (-)
L2
L4
D1 adult
D
Reporter #7
# of RFP+ cholinergic MNs
E
Reporter #8
LIN-39 site mut
D3 adult
F
Endogenous cfi-1 reporter
G
Time
cfi-1 initiation
cfi-1 maintenance
Initiation factor
Hox
X
cfi-1
Enhancer
C03C11.1
~ 12 kb
GATTGATG
LIN-39 binding site
Maintenance factor
UNC-3
UNC-3 binding site

Figure 5 - figure supplement 1

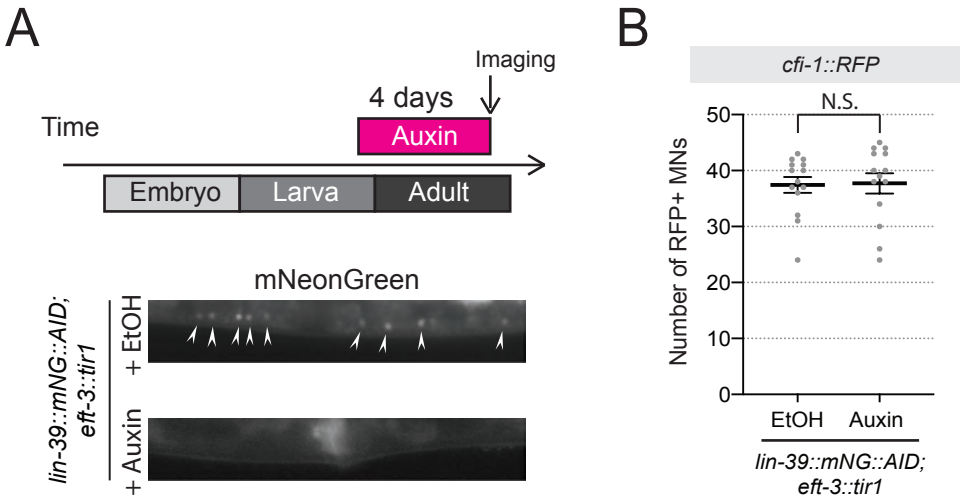

Figure 5 - figure supplement 2

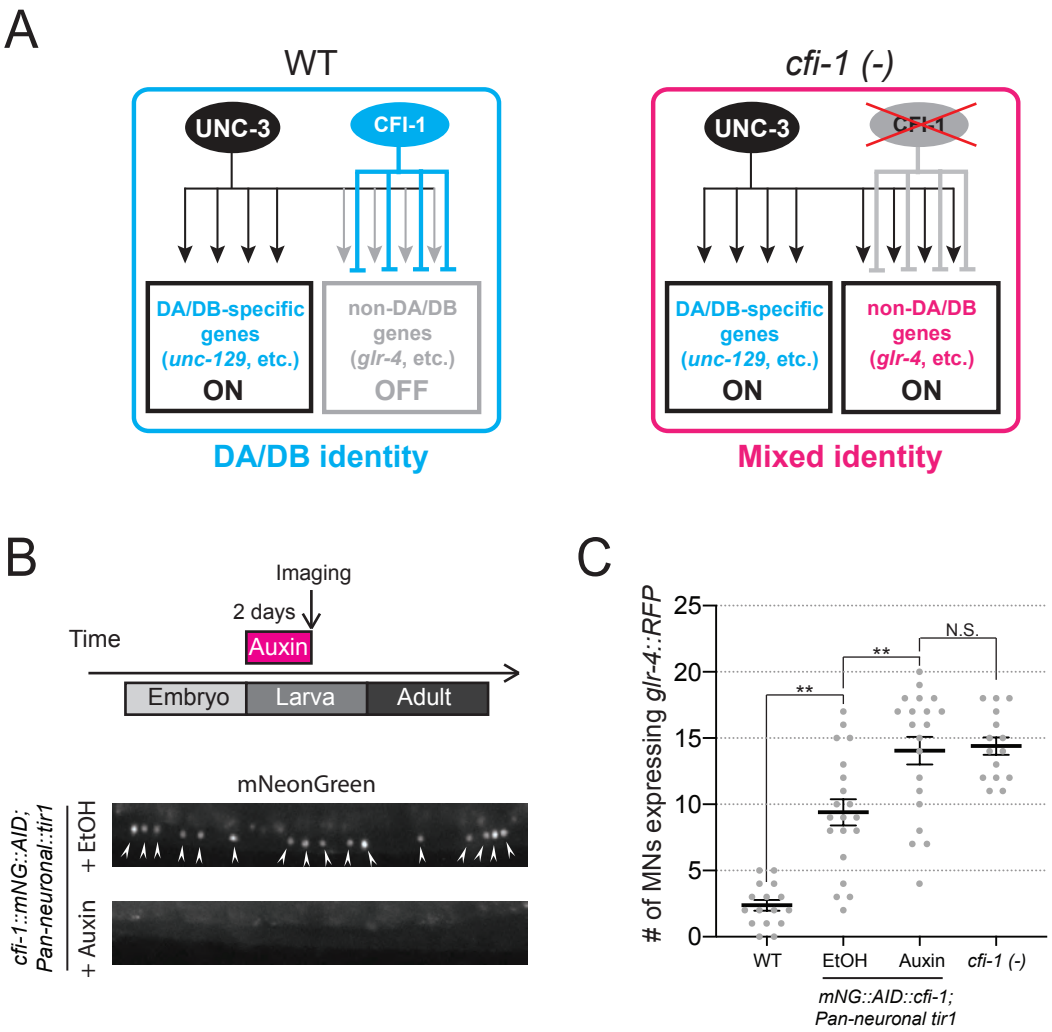

Figure 5 - figure supplement 3

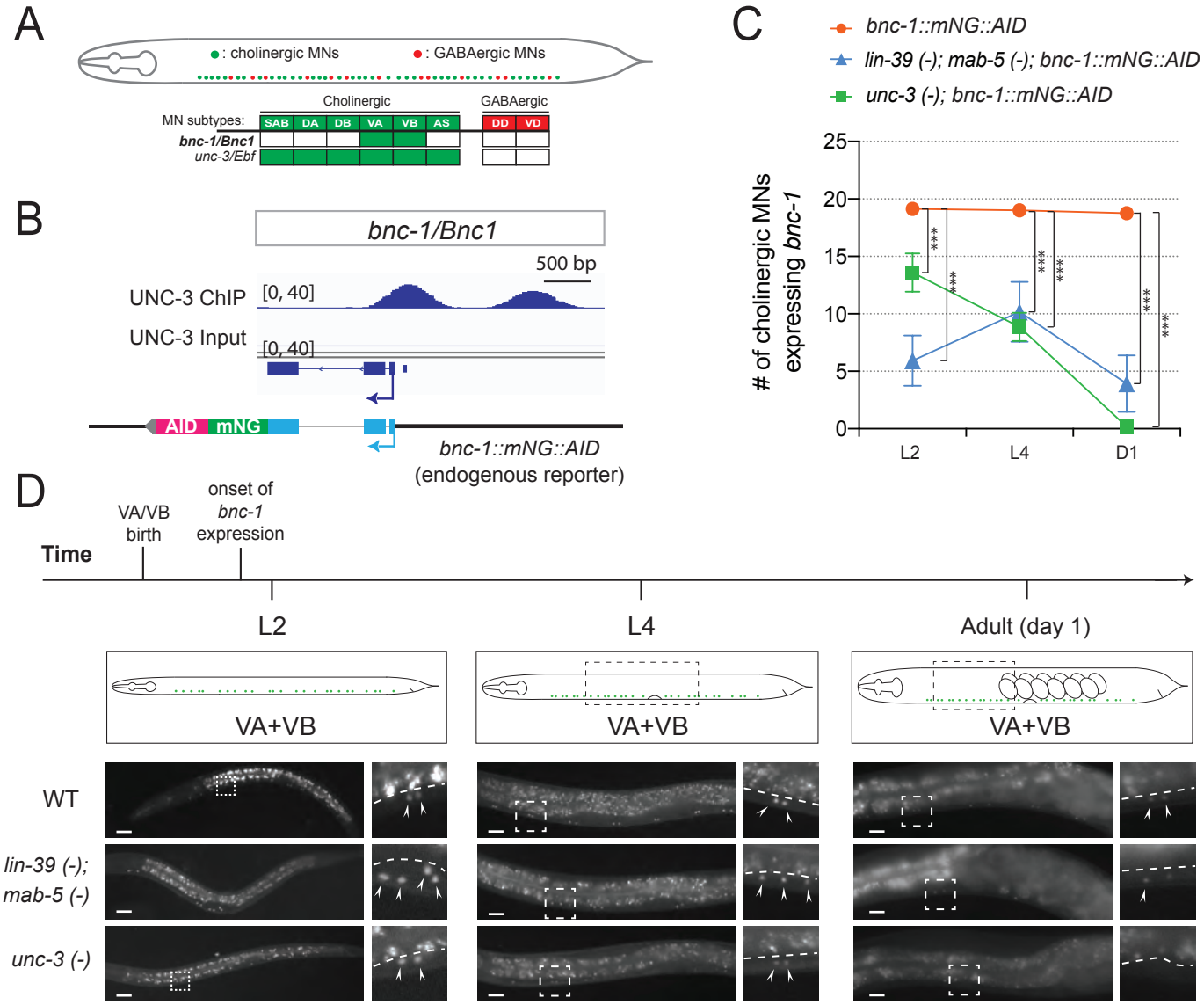

Li_Figure 6

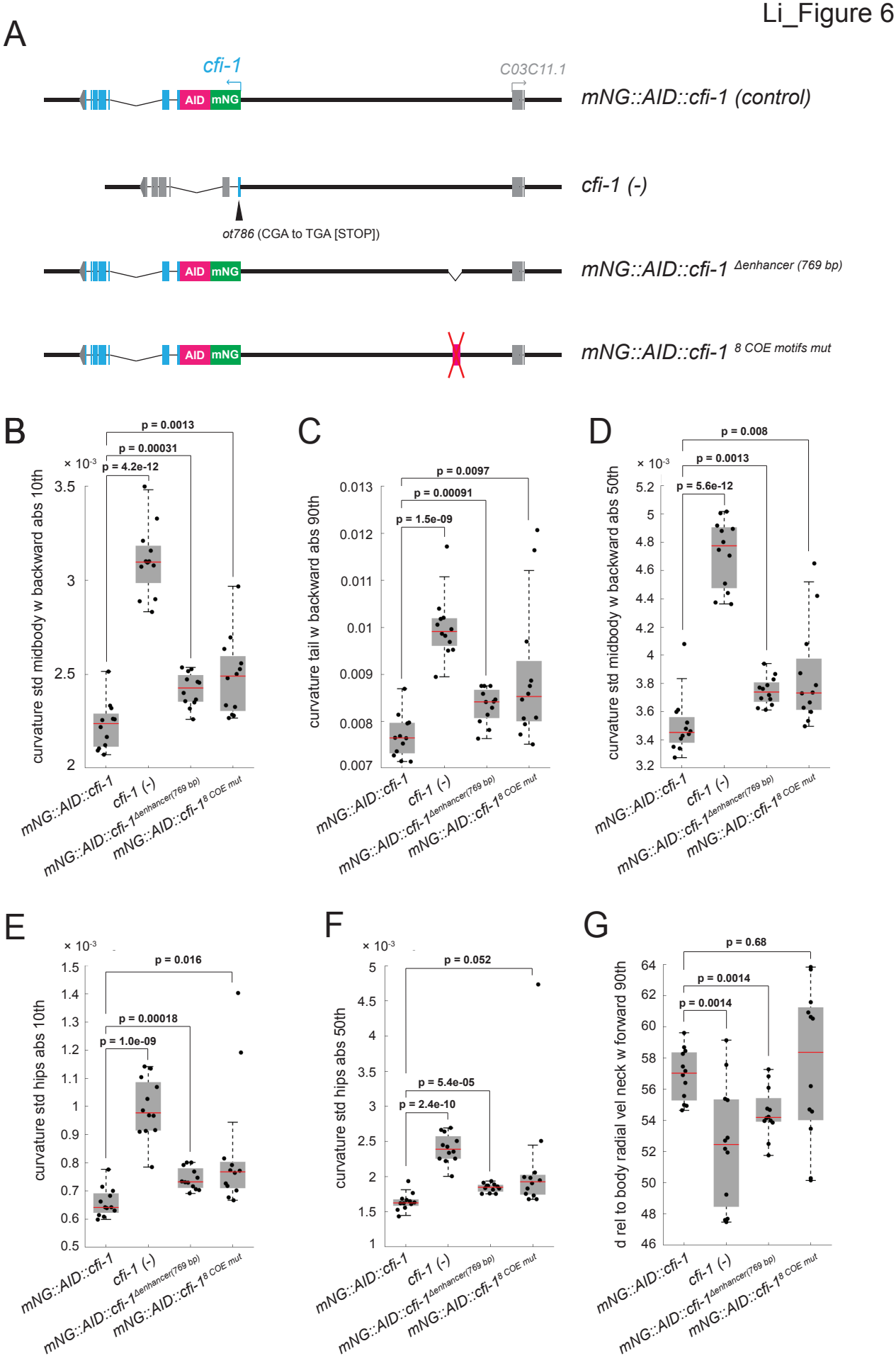
A
cfi-1
C03C11.1
AID
mNG
mNG::AID::cfi-1 (control)
cfi-1 (-)
ot786 (CGA to TGA [STOP])
mNG::AID::cfi-1 Δenhancer (769 bp)
mNG::AID::cfi-1 8 COE motifs mut
B
curvature std midbody w backward abs 10th
× 10-3
p = 0.0013
p = 0.00031
p = 4.2e-12
C
curvature tail w backward abs 90th
p = 0.0097
p = 0.00091
p = 1.5e-09
D
curvature std midbody w backward abs 50th
p = 0.008
p = 0.0013
p = 5.6e-12
E
curvature std hips abs 10th
p = 0.016
p = 0.00018
p = 1.0e-09
F
curvature std hips abs 50th
p = 0.052
p = 5.4e-05
p = 2.4e-10
G
d rel to body radial vel neck w forward 90th
p = 0.68
p = 0.0014
p = 0.0014
mNG::AID::cfi-1
cfi-1 (-)
mNG::AID::cfi-1Δenhancer(769 bp)
mNG::AID::cfi-18 COE mut

Li_Figure 7

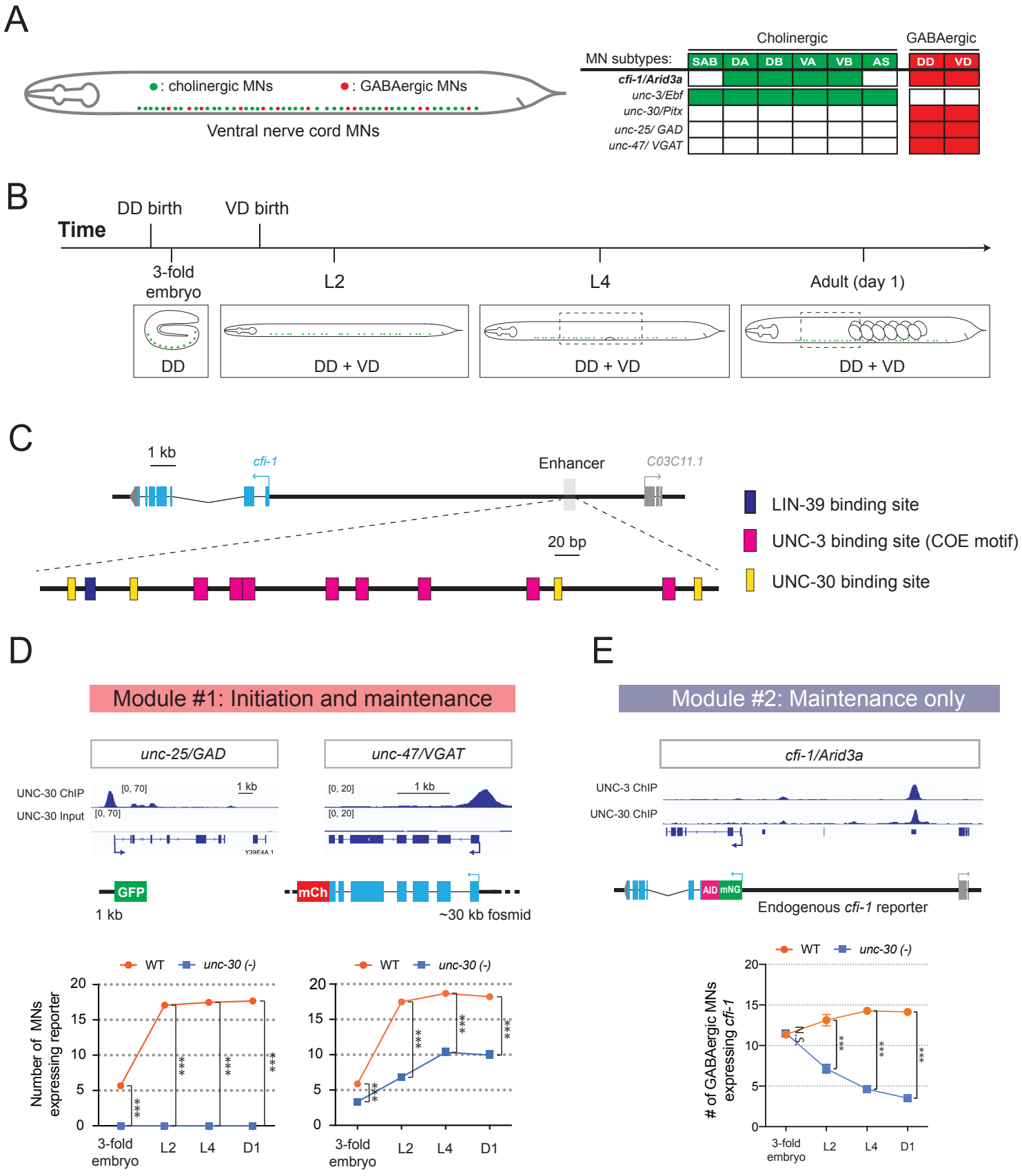
A
: cholinergic MNs
: GABAergic MNs
Ventral nerve cord MNs
Cholinergic
GABAergic
MN subtypes:
SAB
DA
DB
VA
VB
AS
DD
VD
cfi-1/Arid3a
unc-3/Ebf
unc-30/Pitx
unc-25/ GAD
unc-47/ VGAT
B
Time
DD birth
VD birth
3-fold embryo
L2
L4
Adult (day 1)
DD
DD + VD
DD + VD
DD + VD
C
1 kb
cfi-1
Enhancer
C03C11.1
20 bp
LIN-39 binding site
UNC-3 binding site (COE motif)
UNC-30 binding site
D
Module #1: Initiation and maintenance
unc-25/GAD
unc-47/VGAT
UNC-30 ChIP
UNC-30 Input
[0, 70]
[0, 70]
1 kb
[0, 20]
[0, 20]
1 kb
GFP
1 kb
mCh
~30 kb fosmid
WT
unc-30 (-)
Number of MNs expressing reporter
3-fold embryo
L2
L4
D1
E
Module #2: Maintenance only
cfi-1/Arid3a
UNC-3 ChIP
UNC-30 ChIP
AID
mNG
Endogenous cfi-1 reporter
WT
unc-30 (-)
# of GABAergic MNs expressing cfi-1
N.S.
3-fold embryo
L2
L4
D1

Table 1: A summary of the *cis*-regulatory analysis to identify novel transcription factors controlled by UNC-3. Reporter alleles of each TF were built and examined for expression pattern. TFs that are expressed in MNs were further tested for UNC-3 dependency. Ten of 16 tested TFs (62.5%) show expression in MNs, of which 9 require UNC-3 activity for normal expression. Two reporters were generated for *nhr-1* and *nhr-40* because two distinct UNC-3 ChIP-Seq peaks were found in the *cis*-regulatory region of these genes. N/A: Not applicable.

	Reporter	TF family	*cis*-regulatory region included	RFP expression	*unc-3* dependence	Expression	Expression in Cholinergic MNs	Expression in GABAergic MNs	# of lines
1	*nhr-1* (second peak)	Nuclear hormone receptor	-838 bp ~ 1,535 bp	YES	Positively regulated	VNC, Head and Tail Neurons	YES	YES	2
2	*nhr-40* (second peak)	Nuclear hormone receptor	4,356 bp ~ 5,525 bp	YES	Positively regulated	VNC, Head and Tail Neurons	YES	YES	2
3	*mab-9*	T-box	-5,561 bp ~ -3,773 bp	YES	Positively regulated	VNC, Head and Tail Neurons	YES	YES	2
4	*ztf-26*	Zinc finger	910 bp ~ 3,394 bp	YES	Positively regulated	VNC and Head Neurons	YES	NO	2
5	*ceh-44*	C. elegans homeobox	1,605 bp ~ 3,111 bp	YES	Positively regulated	VNC, Head and Tail Neurons	YES	Not determined	2
6	*zfh-2*	Zinc finger	12,048 bp ~ 13,549 bp	YES	Positively regulated	VNC, Head and Tail Neurons	YES	NO	2
7	*cfi-1*	AT-rich interaction domain	-13,824 bp ~ -11,329 bp	YES	Positively regulated	VNC, Head and Tail Neurons	YES	YES	2
8	*bnc-1*	Zinc finger	-1,800 bp ~ -1 bp	YES	Positively regulated	VNC and Tail Neurons	YES	NO	2
9	*nhr-49*	Nuclear hormone receptor	-750 bp ~ 75 bp	YES	Negatively regulated	VNC, Head and Tail	NO	YES	2

						Neurons			
10	*nhr-1* (first peak)	Nuclear hormone receptor	-7,452 bp ~ -5,871 bp	YES	Not tested	Head and Tail Neurons	N/A	N/A	2
11	*nhr-19*	Nuclear hormone receptor	1,261 bp ~ 2,294 bp	YES	NO	VNC, Head and Tail Neurons	Not determined	Not determined	2
12	*nhr-40* (first peak)	Nuclear hormone receptor	919 bp ~ 1,839 bp	YES	NO	VNC, Head and Tail Neurons	Not determined	Not determined	2
13	*ccch-3*	Zinc finger	-385 bp ~ -1 bp	YES	Not tested	Head Neurons	N/A	N/A	2
14	*ztf-17*	Zinc finger	-1,031 bp ~ 3 bp	YES	Not tested	Head Neurons, Muscles, and Intestine	N/A	N/A	2
15	*nhr-47*	Nuclear hormone receptor	-675 bp ~ 171 bp	NO	N/A	N/A	N/A	N/A	2
16	*unc-55*	Nuclear receptor	-2,105 bp ~ -1,327 bp	NO	N/A	N/A	N/A	N/A	2
17	*ztf-13*	Zinc finger	-1,392 bp ~ -1 bp	NO	N/A	N/A	N/A	N/A	2
18	*ztf-14*	Zinc finger	-2,087 bp ~ -531 bp	NO	N/A	N/A	N/A	N/A	2